NASA TECHNICAL MEMORANDUM

NASA TM X-1463

NASA TM X-1463

EXPERIMENTAL EVALUATION OF 7.82-INCH- (19.8-CM) DIAMETER THROAT INSERTS IN A STORABLE-PROPELLANT ROCKET ENGINE

by Jerry M. Winter and Donald A. Peterson

Lewis Research Center

Cleveland, Ohio

NATIONAL AERONAUTICS AND SPACE ADMINISTRATION • WASHINGTON, D. C. • APRIL 1968

NASA TM X-1463

EXPERIMENTAL EVALUATION OF 7.82-INCH- (19.8-CM) DIAMETER THROAT INSERTS IN A STORABLE-PROPELLANT ROCKET ENGINE

By Jerry M. Winter and Donald A. Peterson

Lewis Research Center
Cleveland, Ohio

NATIONAL AERONAUTICS AND SPACE ADMINISTRATION

For sale by the Clearinghouse for Federal Scientific and Technical Information
Springfield, Virginia 22151 – CFSTI price $3.00

EXPERIMENTAL EVALUATION OF 7.82-INCH- (19.8-CM) DIAMETER THROAT INSERTS IN A STORABLE-PROPELLANT ROCKET ENGINE

by Jerry M. Winter and Donald A. Peterson

Lewis Research Center

SUMMARY

A total of 14 nozzle throat inserts of 7.82-inch (19.8-cm) diameter were evaluated for use with reinforced plastic thrust chambers. The propellants used were nitrogen tetroxide and a blend of 50 percent hydrazine with 50 percent unsymmetrical dimethylhydrazine. Nominal test conditions were a chamber pressure of 100 psia (689 kN/sq m) and an oxidant-fuel ratio of 2.0.

Primary failure mechanisms were determined for specific materials and design concepts. Detailed failure mechanisms were explored as a means of recommending material and design modifications to improve reliability and performance. Silicon carbide provided erosion protection for 100 seconds of continuous firing. However, both one-piece and segmented silicon carbide inserts failed structurally. Tungsten infiltrated with copper or silver had relatively high resistance to oxidation for approximately 250 seconds of run time. The copper-infiltrated insert was structurally sound after a firing duration of 340 seconds. Careful attention to substrate design and coating techniques appreciably increased the erosion resistance of coated inserts. A preferentially oriented pyrolytic graphite design was partly successful, but, to realize the full potential of this design, additional development work would be required. Only limited correlation between small- and large-size testing was obtained. Generally, coated inserts were much more successful in small-scale than in large-scale tests. However, the time to failure for large-scale monolithic inserts was extended over small-scale inserts.

INTRODUCTION

Ablative thrust chambers are being used or proposed for a wide range of applications. The inherent simplicity and potential reliability of ablative chambers as compared with regenerative cooling concepts are attractive to design and mission analysis

engineers. Ablative chambers also may be throttled over a wider range than regenerative chambers. Reinforced ablative plastics have been effectively used for both liquid thrust chambers and solid-propellant rocket nozzles at all thrust levels tested to date. Present ablative rocket engines require a compromise between operating efficiency and ablative erosion rate for a given duty cycle. Performance degradation due to throat erosion is most severe for small reaction control-type engines and may be significant in larger engines where maximum available efficiencies and lifetimes are required. Techniques for optimization of reinforced plastic ablative materials for a given environment are briefly discussed in reference 1.

A satisfactory throat insert would eliminate or minimize throat erosion to permit increased engine efficiency or longer engine life or both. To improve the performance and extend the application of ablative thrust chambers, an experimental investigation was undertaken which involved the substitution of throat inserts for the ablative material in the throat region. However, many problems, such as fabrication difficulties, weight, and environmental definition within the thrust chamber itself, must be recognized and resolved.

An experimental investigation with a small-scale engine (throat diam, 1.2 in. or 3.05 cm) was conducted to define some of the material and design problems associated with throat inserts (ref. 2). The present investigation explored some of the primary failure mechanisms of intermediate-size throat inserts (throat diam, 7.82 in. or 19.8 cm). A secondary objective was to compare the results with those from the small-scale program and determine the influence, if any, of scale on failure modes. In the design of the throat insert configuration for the present investigation, problems of oxidation, thermal shock, and thermal stress were considered with respect to particular material and design concepts. The design objective was to eliminate or decrease throat erosion by surface temperature control, boundary-layer injection, variation in material wall thicknesses, or coating technique. A detailed examination of failure mechanisms and nozzle material suitability is given in reference 3.

The propellants used for the test series were nitrogen tetroxide (N_2O_4) and a blend of 50 percent hydrazine (N_2H_4) and 50 percent unsymmetrical dimethylhydrazine (UDMH). Nominal test conditions were a chamber pressure of 100 psia (689 kN/sq m) and an oxidant-fuel ratio of 2.0 with a characteristic velocity efficiency above 96 percent of theoretical equilibrium. A design objective of 300 seconds of continuous firing with restart capability was chosen as a desirable duty cycle. An expansion area ratio of 2.0 used with a 7.82-inch (19.8-cm) throat diameter provided a nominal vacuum thrust level of 7000 pounds force (31.1 kN).

A total of 14 separate throat inserts were tested (2 were modifications of an infiltrated tungsten design), all within an ablative reinforced plastic chamber. Materials tested were

(1) Monolithic silicon carbide
(2) Segmented, thin-wall silicon carbide
(3) Silver-infiltrated tungsten
    (a) Thick wall
    (b) Thin wall
(4) Copper-infiltrated tungsten
    (a) Thick wall
    (b) Thin wall
(5) 0.050-Inch (0.127-cm) pyrolytic graphite coating
(6) 0.100-Inch (0.254-cm) pyrolytic graphite coating
(7) 0.010-Inch (0.0254-cm) pyrolytic graphite coating (heat treated)
(8) 0.010-Inch (0.0254-cm) pyrolytic graphite coating
(9) 0.010-Inch (0.0254-cm) pyrolytic graphite and boron coating (heat treated)
(10) 0.040-Inch (0.1016-cm) pyrolytic silicon carbide coating
(11) 0.005-Inch (0.0127-cm) silicon carbide diffusion coating
(12) Preferentially oriented pyrolytic graphite

The results are presented in groups of the materials tested as follows:

(1) Silicon carbide inserts
(2) Infiltrated tungsten inserts
(3) Coated inserts
(4) Pyrolytic graphite insert

Each insert is discussed individually in detail. Comparisons between all tested materials are made and failure mechanisms discussed. Motion-picture supplement C-255 has been prepared and is available on loan to aid in the analysis. A request card and a description of the film are included at the back of this report.

APPARATUS

FACILITY

The investigation was conducted in an altitude chamber. The overall arrangement of the facility is shown in figure 1. Figure 2 illustrates the mounting of a thrust chamber in the test stand. The weight of the engine was supported by flexure plates which allowed freedom of motion for thrust measurement. Engine exhaust products were passed through a water-cooled collector and cooled by heat exchangers before being exhausted to the atmosphere.

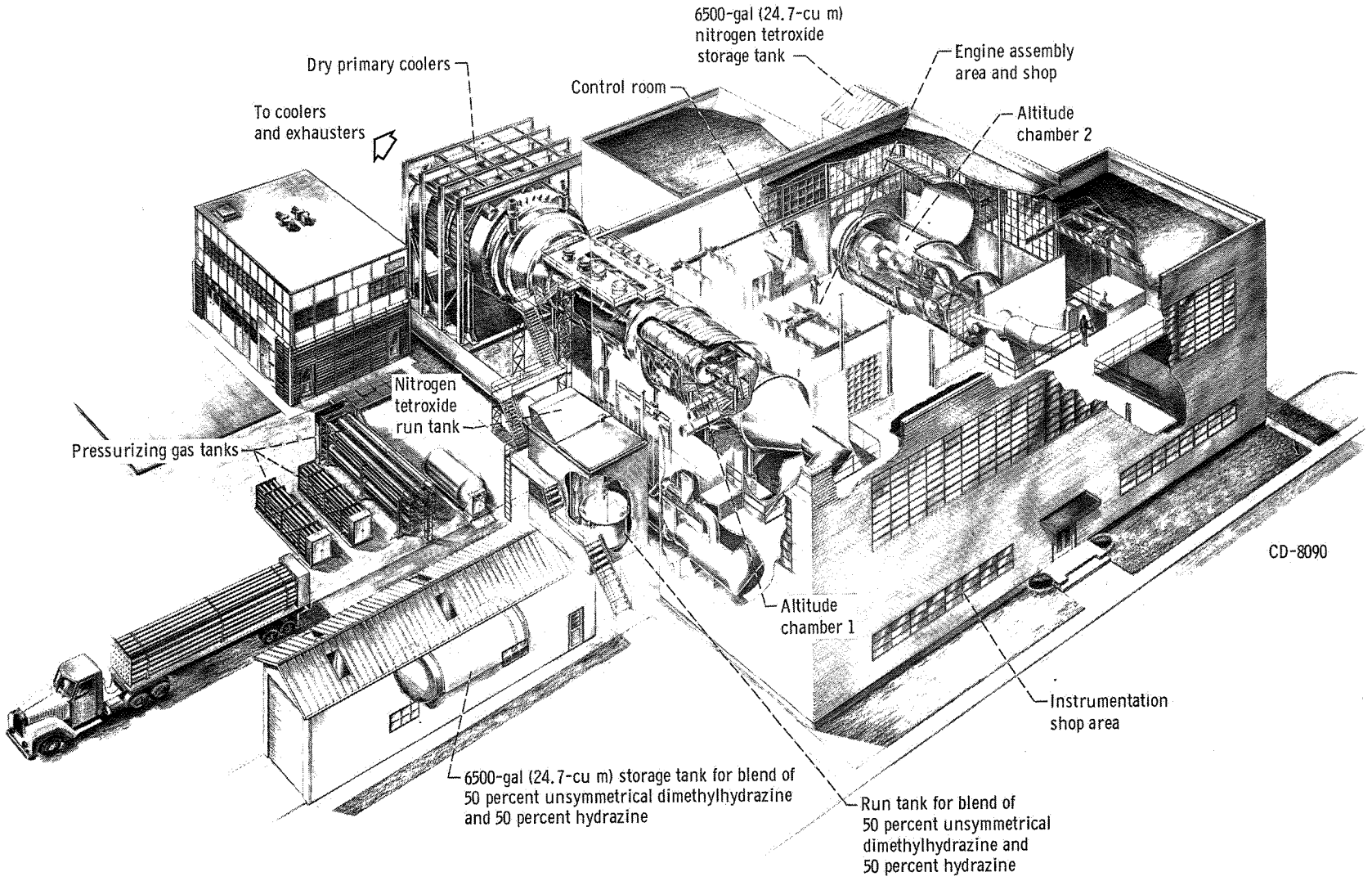

Figure 1. - Altitude facility.

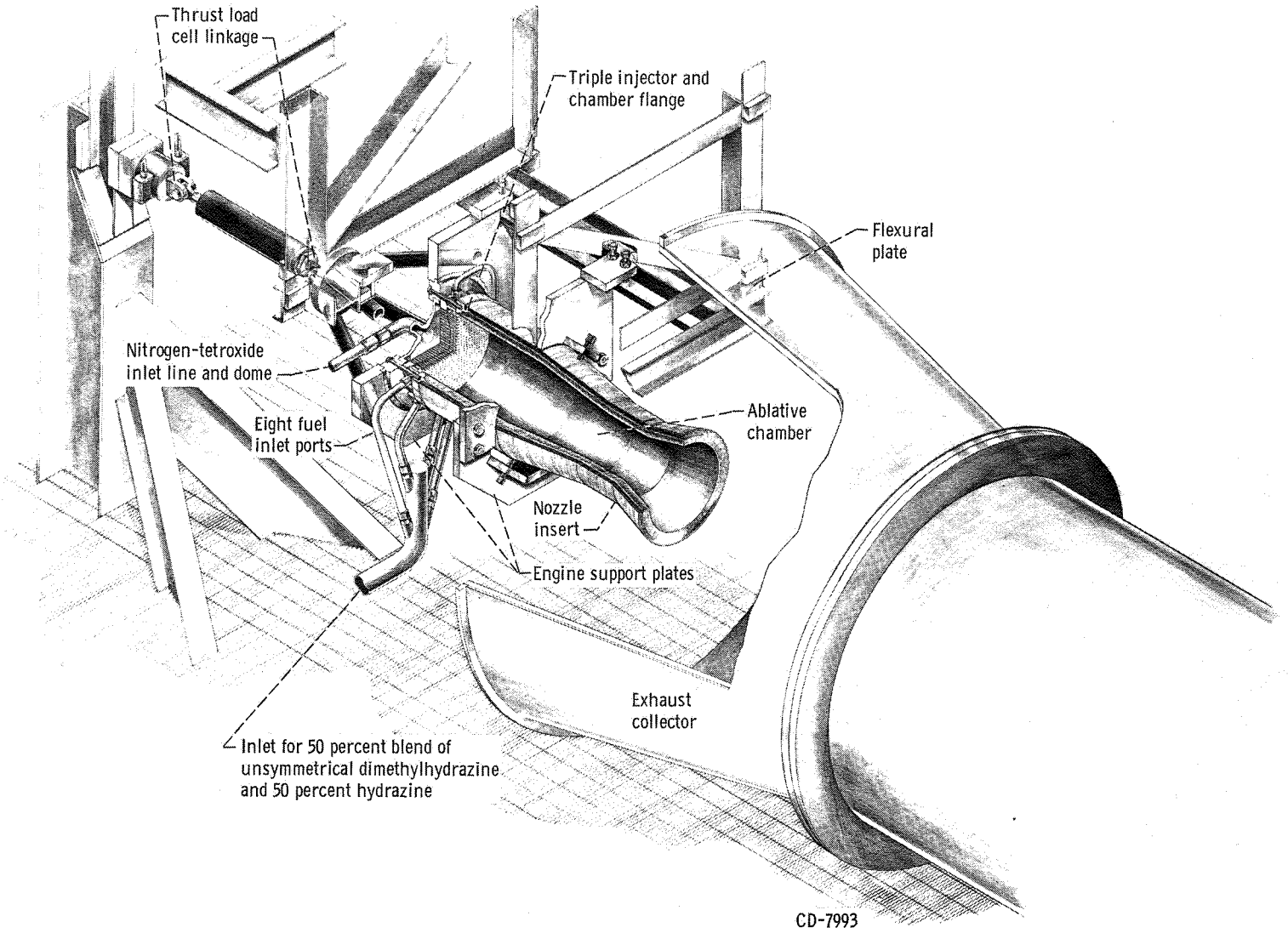

Figure 2. - Ablative chamber and injector; general engine test arrangement.

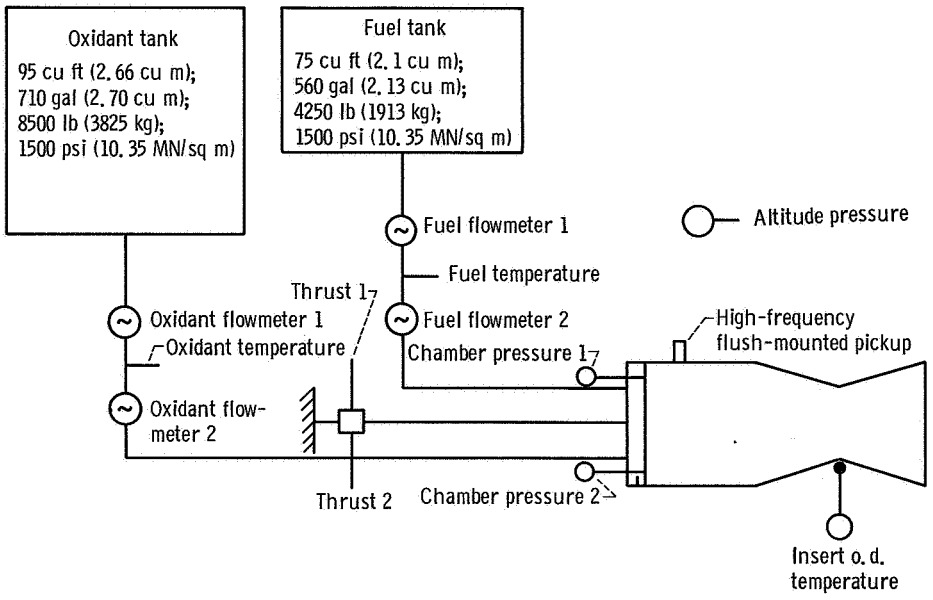

Figure 3. - Flow diagram and instrumentation.

Figure 3 is a schematic diagram showing the flow system and the location of the measured parameters. Two flowmeters in series were used in each propellant line. The propellant tanks were located externally to the test cell in a controlled temperature environment (fig. 1). Propellant tanks initially used in the test program provided 100 seconds of continuous firing. Larger tanks (figs. 1 and 3), installed for the majority of the insert tests, provided continuous run durations in excess of 300 seconds, if no throat erosion occurred.

ROCKET ENGINE ASSEMBLY

The four injectors used for the test program are shown in figures 4 to 7. A description of each injector is given in table I. Injector 1 was used initially because of its availability and high characteristic velocity efficiency. Because of extended use on prior test programs, deterioration of the injector elements occurred after testing insert 1 which necessitated the use of the other injectors. Injector 1 consisted mainly of mutually perpendicular fuel-on-oxidant triplet elements arranged in a grid pattern. The outer elements were showerheads with some excess fuel. The larger circles in figure 4 are the showerhead oxidant elements. The mixture ratio distribution for injector 1 is given in table I.

Injectors 2, 3, and 4 were 127-element fuel-on-oxidant triplets with most of the elements arranged in circular rows with each element lying along a chamber radius. Injectors 3 and 4 had 24 triplets arranged at a 40^{o} angle to a chamber radius. Injectors 2, 3, and 4 were considered to be essentially the same design. Three different injectors were

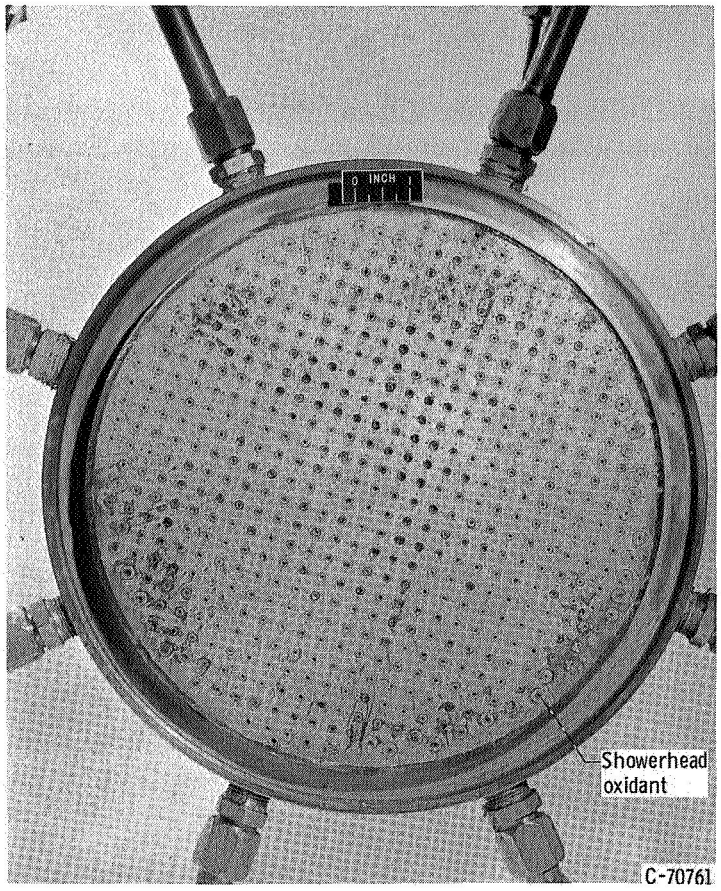

Figure 4. - Injector 1.

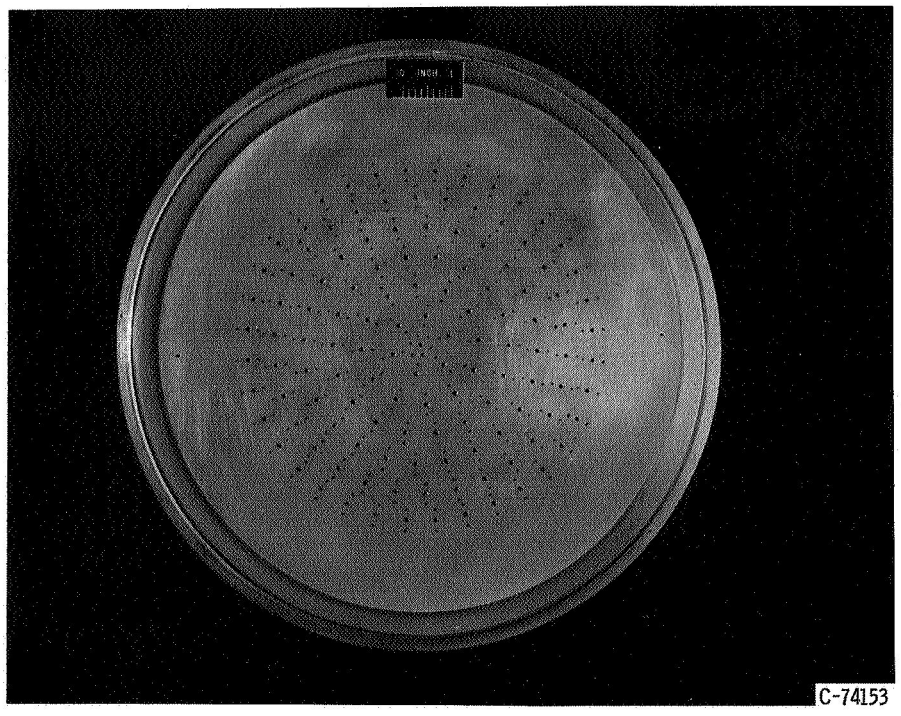

Figure 5. - Injector 2.

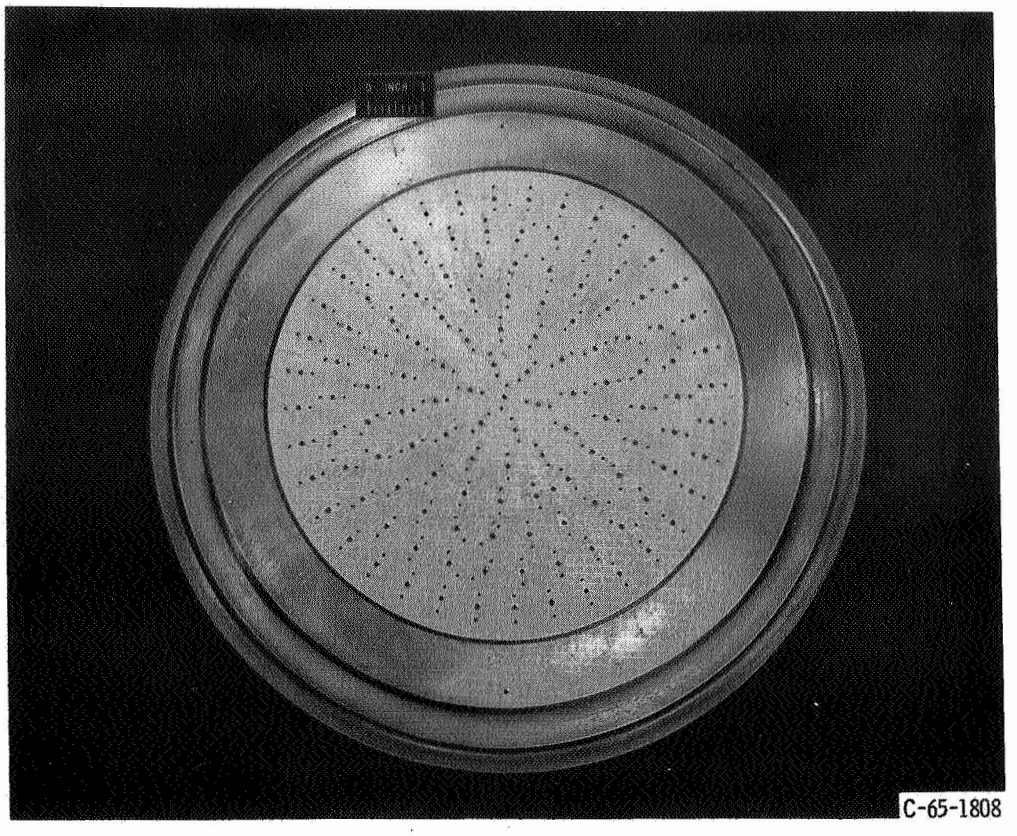

Figure 6. - Injector 3.

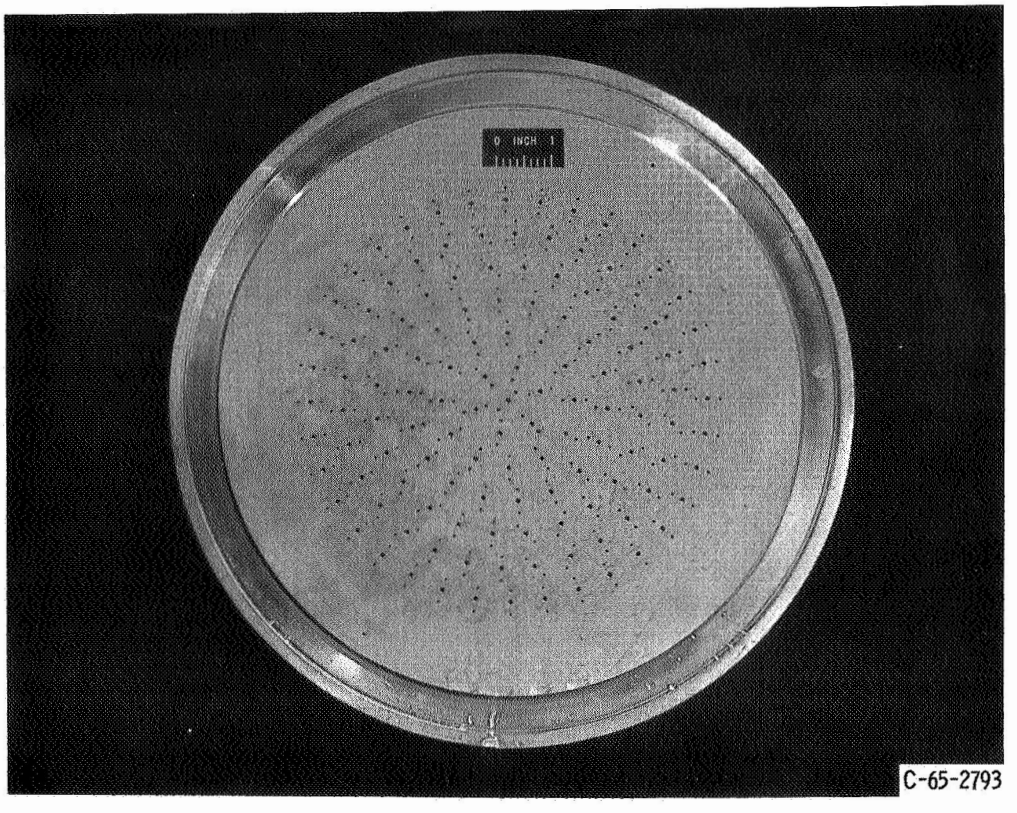

Figure 7. - Injector 4.

TABLE I. - INJECTOR DESCRIPTION

Injector	Pattern	Type	Face material	Oxidant elements			Fuel elements			Impingement			Oxidant-fuel ratio distribution based on area at an overall O/F of 2.0	Percent of total fuel flow
				Number	Size		Number	Size		Distance		Included angle, deg		
					in.	cm		in.	cm	in.	cm			
1	Grid	Triplet (Fuel on oxidant)	Nickel	481	0.035	0.089	962	0.018	0.046	0.578	1.47	30	2.1	81.0
		Showerhead	Nickel	72	0.035	0.089	198	0.018	0.046	-----	----	--	1.5	16.6
		Film cooling	Nickel	---	------	-----	8 8	0.020 .028	0.051 .071	Tangential			All fuel	2.4
2	Circular	Triplet (Fuel on oxidant)	Aluminum	127	0.0785	0.20	254	0.043	0.11	0.56	1.42	40	2.0	100
3	Circular	Triplet (Fuel on oxidant)	Aluminum	127	0.0785	0.20	254	0.043	0.11	0.56	1.42	40	2.0	100
4	Circular	Triplet (Fuel on oxidant)	Aluminum	127	0.0785	0.20	254	0.043	0.11	0.56	1.42	40	2.0	100

required because the particular construction used allowed intermanifold leaks after a number of test firings. These were repaired when possible and the injector was discarded when repairs were not feasible.

Heat sink chambers (fig. 8) were used to evaluate combustion performance during short calibration firings. Performance was measured both with and without a forward water-cooled chamber section.

Sketches and dimensions of chambers used for each insert tested are given in figure 8. Figure 8(c) illustrates application of throat inserts to existing ablative chambers such as were used in reference 4. A total of 10 of the inserts were tested with a forward water-cooled chamber section as shown in figure 8(d).

INSTRUMENTATION

The location of all measured variables are shown in figure 3 (p. 4). Pressure measurements were made with standard strain-gage element transducers. Electrical calibrations were made before and after each test with the use of calibration information from laboratory standard tests. Thrust measurement was made with a double-bridge strain-gage load cell in compression. Calibration was accomplished by loading the cell hydraulically with the engine in place and measuring the true load with a proving ring calibrated by the National Bureau of Standards. Propellant flows were measured with turbine-type flowmeters. Calibrations from water flow measurements were used for the fuel meters while calibrations based on actual nitrogen tetroxide flow were used for the oxidant meters. Propellant flow temperatures were measured with iron-constantan thermocouples referenced to a 150° F (340° K) oven.

PROCEDURE

ENGINE OPERATION AND CONTROL

The altitude chamber pressure was set at 1.74 psia (12.0 kN/sq m) prior to each firing. This level was so selected to match the facility altitude capacity to the engine flow rate that no significant altitude change occurred during the test firing. The propellant tanks were pressurized with nitrogen gas. An automatic closed loop controller was set to provide a constant chamber pressure of 100 psia (689 kN/sq m) and a constant oxidant-fuel ratio of 2.0 for the duration of each firing. Thus, if throat erosion occurred, the propellant flow rate was increased to maintain constant chamber pressure. The firing duration was determined by propellant capacity, insert failure, or an arbitrarily selected time. A high-frequency flush-mounted pressure transducer located in

Engine	D_c		L_{cy}		L_{co}		D_1		D_2		D_t		D_{ex}		ϵ	L^*		β, deg	α, deg
	in.	cm	in.	cm	in.	cm	in.	cm	in.	cm	in.	cm	in.	cm		in.	cm		
A: Water cooled with heat sink	10.78	27.40	19.12	48.6	25.0	63.5	-----	-----	----	-----	7.82	19.85	11.0	27.9	1.98	45.3	115.2	15	15
B: Heat sink	10.78	27.40	23.23	59.0	28.9	73.4	-----	-----	----	-----	7.82	19.85	8.92	22.65	1.30	53.0	134.6	15	15
	10.78	27.40	23.23	59.0	25.9	65.75	-----	-----	----	-----	7.82	19.85	8.92	22.65	1.30	42.0	106.7	15	15
C: 1	10.78	27.40	13.50	34.3	25.0	63.5	8.46	21.5	8.56	21.7	7.82	19.85	11.0	27.9	1.98	41	104.1	8.00	15
C: 2	10.78	27.40	13.50	34.3	25.0	63.5	8.46	21.95	8.56	21.7	7.82	19.85	11.0	27.9	1.98	41	104.1	7.66	15
D: 3, 3a, 4, 4a, 5, 7, 8, 9, and 11	10.78	27.40	12.00	30.5	21.0	53.4	9.50	24.10	8.60	21.85	7.82	19.85	9.5	24.10	1.48	38	96.5	22-25	15
D: 10 and 6	10.78	27.40	12.00	30.5	22.5	57.2	10.78	27.4	8.60	21.85	7.82	19.85	9.5	24.10	1.48	39	99.0	24	15
D: 12	10.78	27.40	12.00	30.5	21.8	55.4	10.78	27.4	8.60	21.85	7.82	19.85	9.9	25.15	1.60	39	99.0	23	15

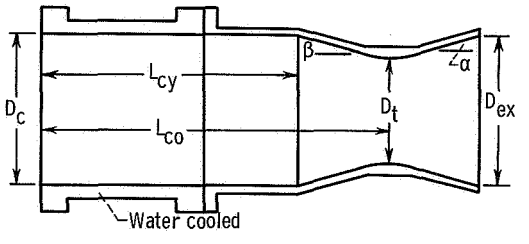

(a) Water cooled with heat sink.

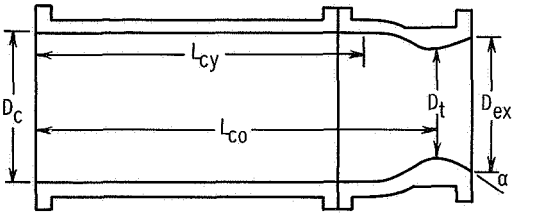

(b) Heat sink chamber and nozzle.

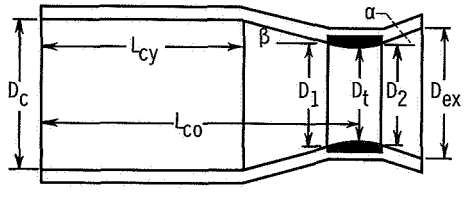

(c) Ablative engine with insert.

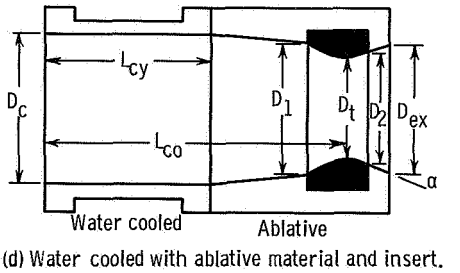

(d) Water cooled with ablative material and insert.

Figure 8. - Combustion-chamber configurations.

the chamber was also monitored with an oscilloscope, and firing was terminated immediately if high-frequency combustion oscillations (screech) were observed. At regular intervals throughout the program, test firings of 6-second duration were made with heat-sink nozzles of fixed geometry to calibrate injector performance.

DATA RECORDING AND PROCESSING

All electrical sensor outputs were sampled at the rate of 4000 samples per second, digitized, and recorded on magnetic tape by the central data recording system. Selected sensor outputs were also recorded by high-speed multichannel oscillograph and strip-chart recording instruments for use in monitoring system operation and for immediate data analysis. The primary digital data were converted into calculated values by use of a digital computer. (The symbols and calculations used are listed in the appendix.)

The primary method for calculating the effective throat radius change ΔR_e was as follows:

$$\Delta R_e = R_t - R_i$$

where the initial radius R_i is that determined by micrometer measurement of the throat insert before any testing and the throat radius R_t is calculated instantaneously by use of the following equation:

$$R_t = \sqrt{\frac{\eta_{C^*} C^*_{theor} w_p}{\pi g P_{c,\,corr} C_d}}$$

Two alternative methods were used to check the calculation: (1) After each firing, the insert throat diameter was measured with a micrometer at 45^o intervals, and the average value was used to calculate the radius change. (2) A photograph of the throat plane of each nozzle was enlarged and the area determined by mechanical integration. This area was then converted to an effective radius from which the effective radius change was calculated. Metallographic analyses of the insert after testing were made when necessary. Post-test photographs were made for each insert.

THEORETICAL STRESS CALCULATIONS

To provide a design guide, theoretical stress calculations were made where the

techniques available were applicable to the materials used. The radial temperature profile at the throat plane was calculated by use of the methods of reference 5. The time of maximum temperature gradient across the throat insert was chosen for calculating the maximum thermal stress across the insert. The method for stress calculation used was that of reference 6, which neglects end effects and assumes that the materials are layerwise elastic, homogeneous, and isotropic and that temperature is independent of axial position. Physical property data were obtained, where possible, from the material suppliers, and extrapolation of the data to high temperature was necessary. A potentially large error in the calculated stress was therefore quite possible.

RESULTS AND DISCUSSION

COMBUSTION ENVIRONMENT

The characteristic velocity efficiency η_{C^*} of each injector, as determined from heat-sink calibration firings, is listed in table II. A total-pressure probe was used to

TABLE II. - INJECTOR PERFORMANCE

Injector	Number of heat-sink calibration firings	Characteristic velocity efficiency (O/F = 2.0), percent	Characteristic velocity efficiency precision, s, percent	Number of insert firings	Insert test time, sec
1	20	98.2	±0.8	5	357
2	17	97.1	±.3	4	359
3	15	97.0	±.3	7	1228
4	4	96.8	±.3	5	553

obtain throat pressure. A correction constant was then obtained which represents the percentage difference from the measured injector end chamber pressure and the measured throat pressure. The η_{C^*} values obtained from both thrust and the corrected chamber pressure were within ±0.10 percent of each other. Values in table II were obtained from thrust measurement. The precision of η_{C^*} is stated in terms of one standard deviation s (the square root of the arithmetic mean of the squares of all the calculated η_{C^*} variations). The number of calibration firings is also listed. No change in the efficiency of any injector was noted during the course of the test program.

Injector 1 was designed to provide an oxidant-fuel ratio O/F of 1.5 on the outer periphery and an O/F of 2.1 in the center with an overall O/F of 2.0. Because of

element deterioration, injector 1 was used to test only one insert.

Injectors 2, 3, and 4 were designed to provide a uniform O/F distribution and did provide a basically identical combustion environment. The 11 inserts tested with these injectors were subjected to essentially the same test conditions.

Table II also lists the number of insert firings and total insert test time for each of the injectors. Some of the inserts were tested with more than one injector. Since three of the injectors were essentially the same, the test results should not be affected.

The test facility enabled steady-state combustion to be reached within 2 seconds of the fire valve opening. The automatic controller enabled the test conditions to be held at a chamber pressure between 99 and 105 psia (682 and 723 kN/sq m) and at an O/F ratio between 1.98 and 2.06 for the duration of all the test firings.

THROAT INSERT RESULTS

All the inserts tested are discussed as groups: silicon carbide inserts, infiltrated tungsten inserts, coated inserts, and a pyrolytic graphite insert. A complete profile, including a detailed sketch, firing data, and postfiring photographs, precedes the group discussions. Each insert is discussed in terms of design, firing results, post-test analysis, comparison with small-scale testing, and correlation with theoretical calculations. A summary of the results for each group is given separately.

Silicon Carbide Inserts

Insert 1: monolithic KT silicon carbide. - Insert 1 was monolithic silicon carbide designed to fit into an existing ablative thrust chamber. The purpose was to improve the throat erosion resistance over an all-ablative chamber, as reported in reference 4. The insert was designed with a 0.930-inch- (2.36-cm) thick wall at the throat and coated with a zirconia layer 0.050-inch (0.127-cm) thick on the outside (fig. 9(a)). The heavy wall provided heat-sink capacity to keep the inside surface of the silicon carbide below the oxidation temperature. The zirconia layer provided insulation to reduce heat flux to the ablative envelope and an expansion seal of 0.020-inch- (0.0508-cm) thick polytetrafluoroethylene was applied to both ends of the insert to reduce axial restraint and help prevent cracking. The design was intended to survive continuous firing durations of 100 seconds (a propellant tank size limitation early in the program).

Insert 1 was tested with injector 1 because of its availability at the time of the test. The first firing (fig. 9(b)) was ended after 2.6 seconds by a high chamber pressure signal. The test produced a circumferential crack at the insert throat. Three subsequent

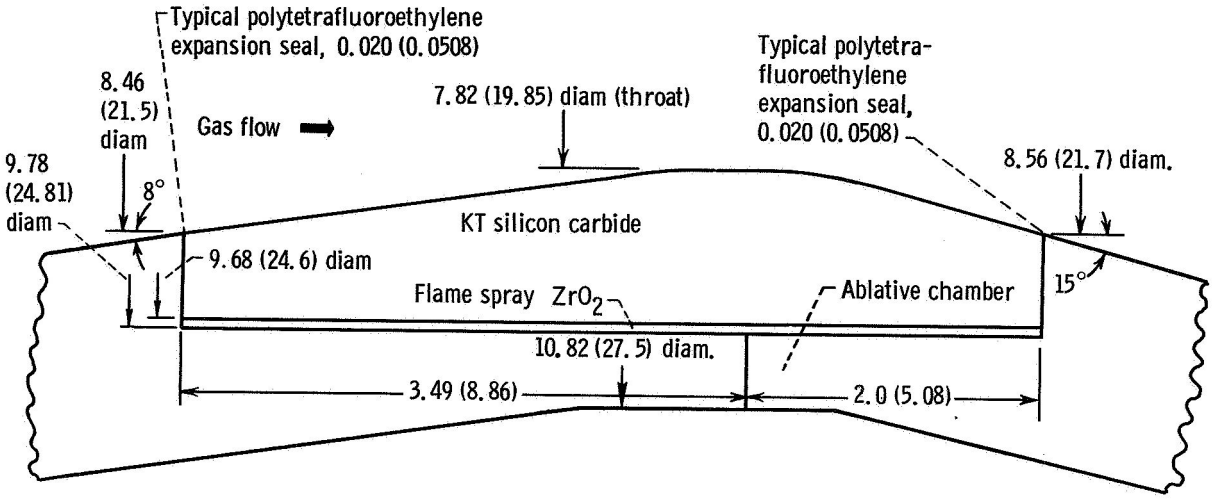

(a) Insert sketch.

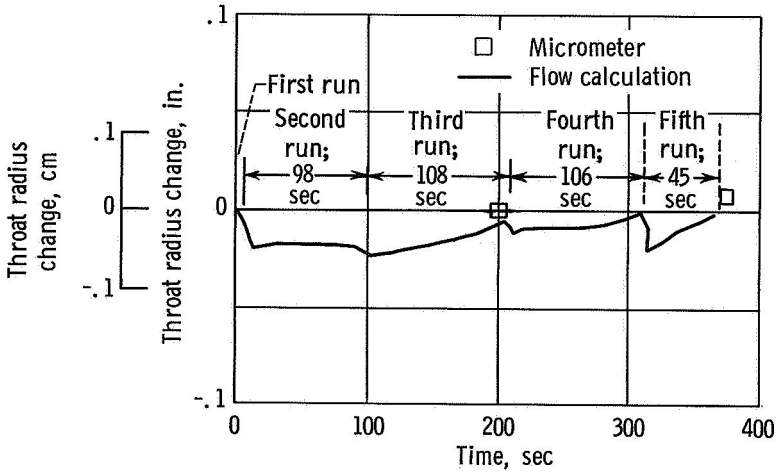

(b) Firing data.

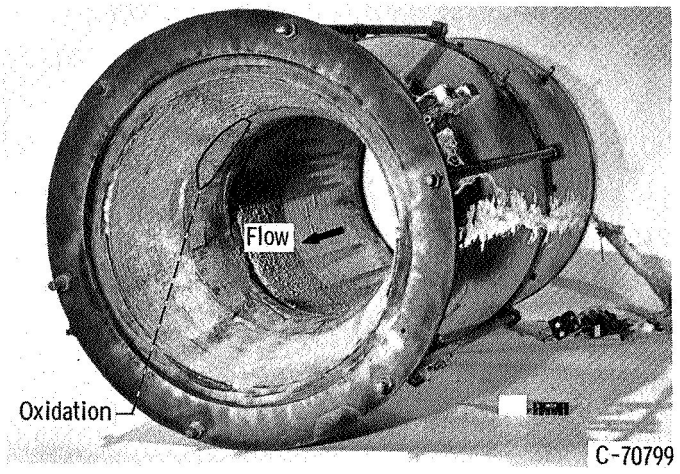

(c) Postfiring photograph.

Figure 9. - Profile of insert 1. (All dimensions not otherwise noted are in inches (cm).)

firings of about 100-second duration each produced increased circumferential and axial cracking but no significant throat erosion (fig. 9(b)) at this point in the test program. Run durations were limited by propellant tank capacity. During the last 100-second firing, cracked pieces of the insert leading edge were ejected which led to burn through of the ablative envelope at the insert leading edge during the final 50-second firing. The extent of insert cracking and material loss is shown in the post-firing photograph of figure 9(c). The silicon carbide insert design did eliminate throat erosion over the 357-second total firing duration, however. The best all-ablative engine from reference 4 had increased 4 percent in throat area after the same total firing duration with the same injector. The polytetrafluoroethylene expansion seals did not prevent insert cracking, but the heavy wall design prevented oxidation of the insert inside surface. The thickness of the zirconia thermal barrier on the insert outside surface was apparently inadequate in reducing the heat load to the ablative envelope. The ablative material around the insert was completely charred following the 357 seconds of total firing. Either a better insulator or a thicker ablative envelope would be required to solve the char-through problem. These, in turn, could lead to higher insert surface temperatures, however.

Unreported Lewis data show that the small-scale testing (1.2-in. or 3.04-cm throat diam) of silicon carbide inserts in a similar combustion environment causes only axial cracks. The thick wall design of the small-scale insert provided retention of the cracked pieces. Failure in the small size was caused by ablative erosion at the insert leading edge and gas flow behind the insert. Loss of insert material due to cracking is a more severe problem in the large-scale insert than in the small-scale insert. The pieces are not keyed together as well in the large-scale insert because of the difference in insert thickness-diameter ratio (0.1 for large scale and 0.4 for small scale). Ablative erosion at the insert leading edge was a problem during extended duration firings in both throat sizes.

A theoretical analysis made after the insert test predicted tensile stresses on the insert outside surface of 42 000 psi (290 MN/sq m) tangentially and 7 000 psi (48.2 MN/sq m) axially. The ultimate tensile strength of KT silicon carbide as reported by the vendor was 25 000 psi (172 MN/sq m). The analysis predicted failure by axial cracking, but the insert actually failed both axially and circumferentially. The most likely sources of error are the 7000 psi (48.2 MN/sq m) axial stress prediction and the possibility that the insert ultimate strength was less than the 25 000 psi (172 MN/sq m) in the axial direction. The strength uniformity would be a function of the manufacturing techniques complicated by the large size of the insert.

Insert 2: segmented, thin-wall KT silicon carbide. - Insert 2, segmented, thin-wall silicon carbide, was also designed to fit into an existing ablative thrust chamber. Based on the experience with insert 1, insert 2 was segmented as shown in figure 10(a). In addition, the wall thickness was reduced from 0.930 to 0.375 inch (2.36 to 0.953 cm) at

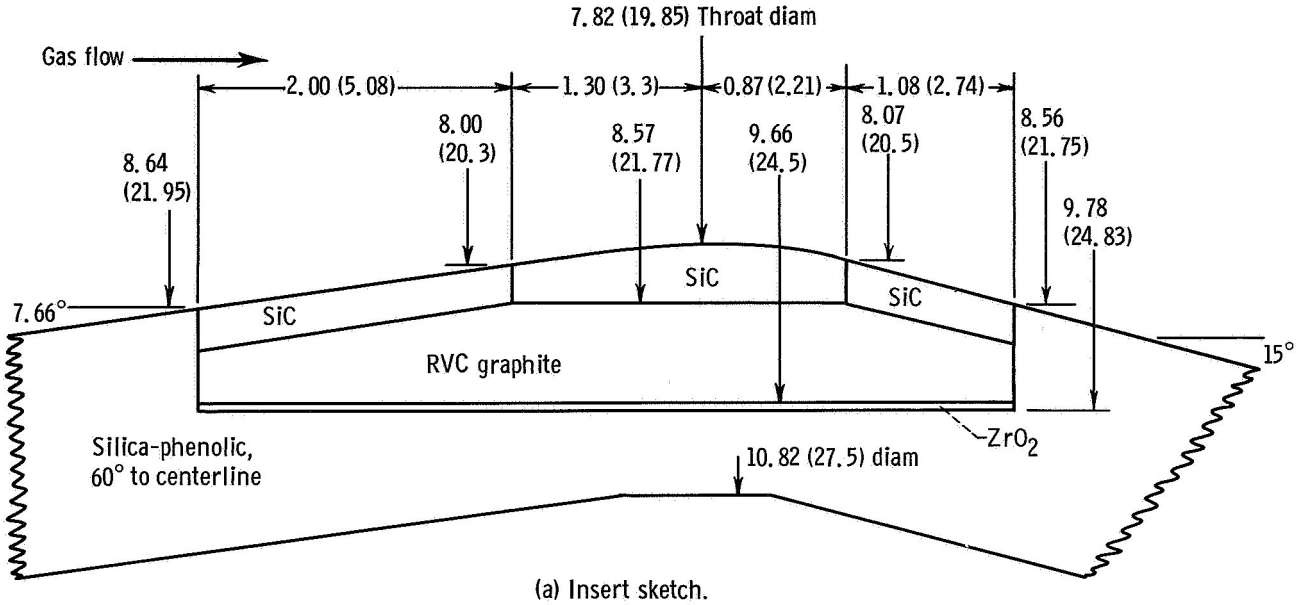

(a) Insert sketch.

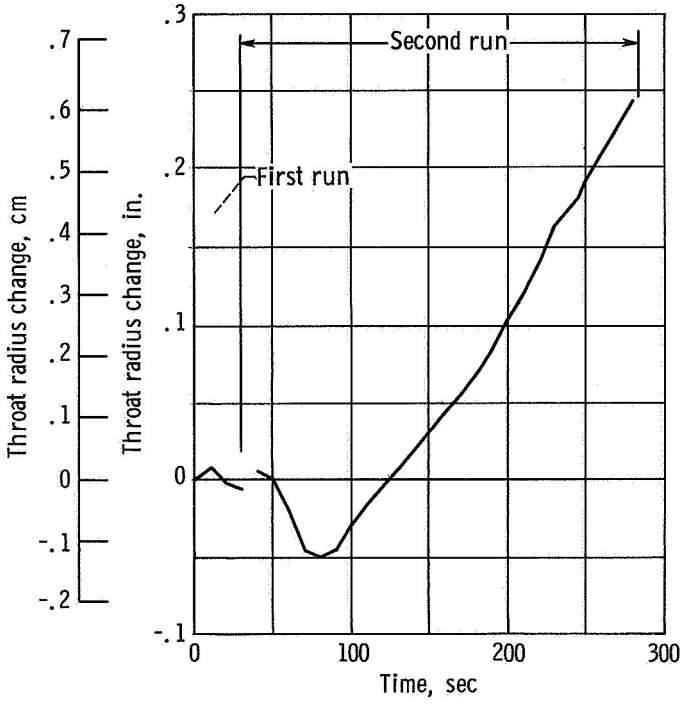

(b) Throat erosion.

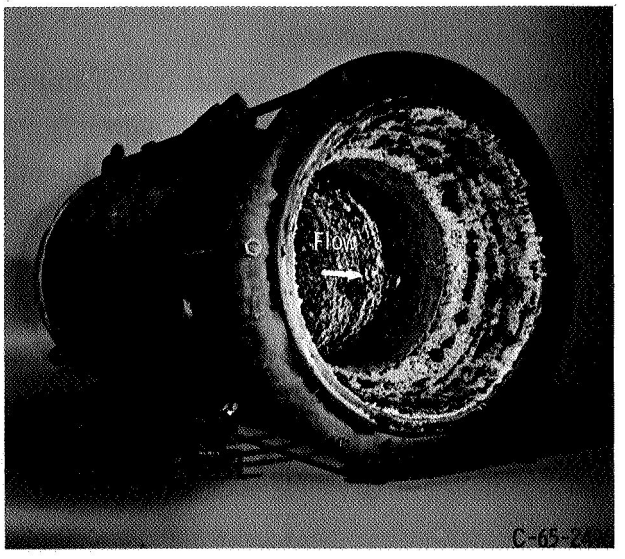

(c) Post-test photograph.

Figure 10. - Profile of insert 2. (All dimensions not otherwise noted are in inches (cm).)

the throat. The axial segments were designed to prevent circumferential cracking. Segment lengths were chosen to include all the curvature in the throat segment and to make the other segments straight tapers. Thermal stresses were calculated at a tension of 5000 psi (34.45 MN/sq m) on the insert outer surface with the 0.375-inch-(0.953-cm) thick wall. Since 5000 psi (34.45 MN/sq m) was significantly lower than the expected ultimate stress of 25 000 psi (172 MN/sq m), the reduction in wall thickness should have solved the thermal stress problem. The RVC graphite behind the silicon carbide throat insert was designed to provide heat-sink capacity to keep the inside surface of the silicon carbide below the oxidation temperature. The RVC was chosen to match the expansion of silicon carbide. The 0.060-inch (0.152-cm) zirconia layer on the outside of the RVC graphite was to reduce the heat flux to the ablative envelope, and polytetrafluoroethylene tape (0.003 in. or 0.0076 cm thick) was used between each of the insert segments to reduce axial restraint and help prevent cracking. The first firing (fig. 10(b)) of 30 seconds was timed to measure thermal-stress effects on the design. Following the first firing, all segments had at least one circumferential crack, but no axial cracks were noted; a probable need for more axial segments was thus indicated. The second firing of 252 seconds produced the erosion shown in figure 10(b). The firing was terminated by ablative burn-through at the leading edge of the insert. Figure 10(c) shows the post-test condition of the chamber and insert. Axial and circumferential cracks are both present. Loss of insert material at the leading edge obviously contributed to burn-through of the ablative material. A large amount of ablative erosion upstream of the insert, which was partly responsible for the leading edge failure, is evident in figure 10(c). The final profile of the chamber is illustrated in figure 11. The

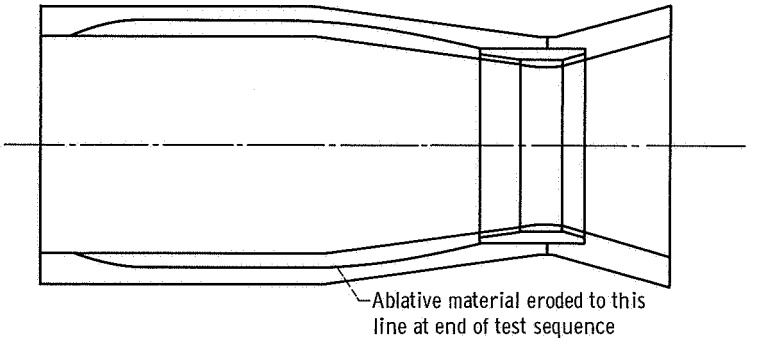

Figure 11. - Ablative erosion associated with insert 2.

ablative erosion was caused by the particular injector (injector 2) and also contributed to insert failure. The large decrease in apparent throat radius during the second firing was due to flow of molten silica from the ablative chamber through the throat. This flow began about 30 seconds into the firing, as illustrated in the film supplement.

The design of insert 2 was not successful in eliminating thermal stress failure but did provide about 100 seconds of operation with no erosion, as with insert 1. The ero-

sion measured was from oxidation due to a combination of silica flow over the silicon carbide insert and also from the propellant combustion products. The ablative material around the insert was completely charred; this charring indicated the end of its useful life.

Unreported Lewis data show that small-scale testing of an axially and circumferentially segmented silicon carbide insert caused only axial cracks. Erosion due to oxidation for a continuous 261-second firing was similar to that reported for insert 2. No loss of material due to cracking was experienced in the small-scale testing. The leading edge failure of insert 2 illustrates the catastrophic results of structural failure in large-scale inserts. Theoretical calculations gave a safety factor of 5 for the insert design, but the insert cracked, regardless. The actual ultimate strength of the insert may have been less than 25 000 psi (172 MN/sq m), and the actual thermal stresses in the insert were probably higher than 5000 psi (34.45 MN/sq m). Possible discrepancies in the analysis include incorrect assumptions such as homogeneity and isotropic behavior or incorrect temperature profiles calculated for the complex insert structure.

Summary. - Inserts 1 and 2 both eliminated throat erosion for 100-second continuous firings. However, the structural failure due to thermal stress caused loss of insert material at the leading edge, which, in turn, led to engine burnout. The leading edge of both inserts was placed at a point of relatively high Mach number flow. Ablative erosion at the insert leading edge definitely contributed to failure of the insert-chamber combination. With insert 1, placement of the insert leading edge at the full chamber diameter might have eliminated leading-edge failure. However, with insert 2, the injector used eroded the ablative chamber so severely (fig. 10(c)) that a more compatible injector would be required or a chamber liner used to prevent excessive chamber erosion.

The oxidation of insert 2 during firing beyond 100 seconds continuously could have been caused by any or all of the following:

(1) The heat-sink capacity of the design was only sufficient to hold the temperature below the oxidation threshold for 100 seconds. Heat flow from the silicon carbide to the graphite could have been reduced by insufficient contact between the two surfaces.

(2) Flow of molten silica from the chamber over the insert contributed to oxidation of the silicon carbide.

(3) The combustion environment was more highly oxidizing than anticipated.

Analytical stress techniques which take into account three-dimensional effects, together with more reliable material property data, are a prerequisite for any future design if a reasonable correlation between theory and practice is to be obtained.

Insert 3: thick-wall silver-infiltrated tungsten. - The thick-wall design of insert 3 (fig. 12(a)) was intended to provide a large heat-sink capacity while the silver infiltrant provided additional cooling capacity and ductility. During firing, the silver should absorb heat by changing state. Silver flow into the boundary layer should protect the tungsten from oxidizing combustion products. The tantalum coating on the insert outer surface was to prevent a reaction between the tungsten-silver and the graphite, while the graphite behind the insert provided additional heat-sink capacity. The 0.060-inch-(0.152-cm) thick zirconia on the outside of the graphite was provided to reduce the heat flux to the ablative envelope and hopefully to increase the run duration. A clearance of 0.015 inch (0.0381 cm) between the zirconia and the ablative material was added to allow for differential thermal expansion. A theoretical analysis of the design predicted a maximum 66 000 psi (455 MN/sq m) tension on the outside of the tungsten-silver, and inasmuch as the tungsten-silver insert has a reported ultimate strength of about 70 000 psi (483 MN/sq m) tension, the design was marginal on the basis of thermal stress.

The first firing of insert 3 was ended at 102 seconds because of a propellant tank capacity limitation. No throat erosion or cracking was experienced (see fig. 12(b)). The decrease in throat radius was due, in part, to molten silica from the upstream ablative material flowing over the throat insert. The solidified silica is shown on the insert post-test photograph (fig. 12(c)). The ablative envelope around the insert was badly cracked, however, and some gas leakage had occurred which caused test termination. Metallographic analysis identified the material on the inside surface of the insert as silicon dioxide with slight traces of tungsten trioxide. Ablative cracking due to differential thermal expansion prevented further testing. The insert assembly apparently did not incorporate the intended 0.015-inch (0.0381-cm) expansion gap required to prevent cracking. Small-scale results for tungsten-silver presented in reference 2 show high erosion due to oxidation during two firings totaling 108 seconds. The overall erosion rate was 0.001 inch (0.0025 cm) per second. The marked difference in behavior for the two sizes could be explained by any of the following reasons:

(1) The large insert design had a higher heat-sink capacity, which kept its surface temperature below the oxidation temperature for this particular run duration.

(2) The oxidizing potential was probably greater in the small-scale tests than in the large-scale tests because the small-scale injector had two oxidizer elements impinging on one fuel element, while the large-scale injector had two fuel elements impinging on one oxidizer element.

(3) The silver infiltrant was more effective in protecting the tungsten in the large-scale tests than in the small-scale tests because the volume-to-surface ratio was 50 percent greater in the large-scale than in the small-scale tests.

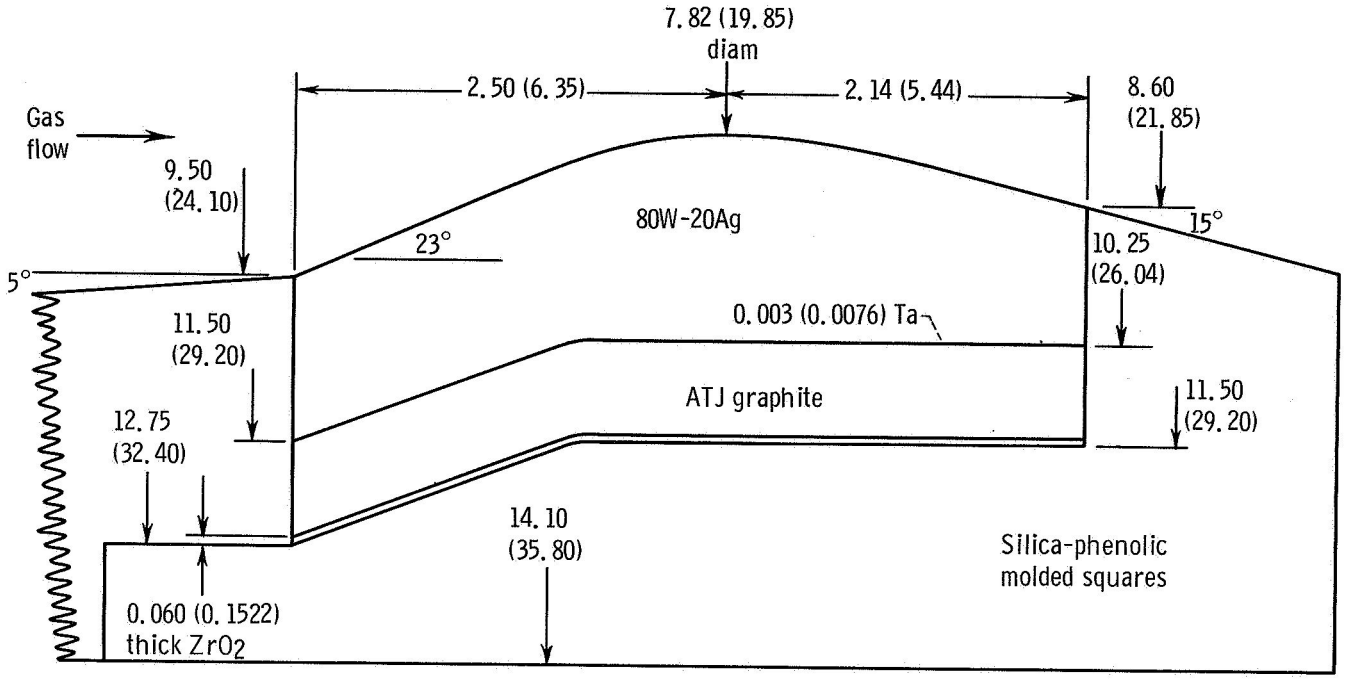

(a) Insert sketch.

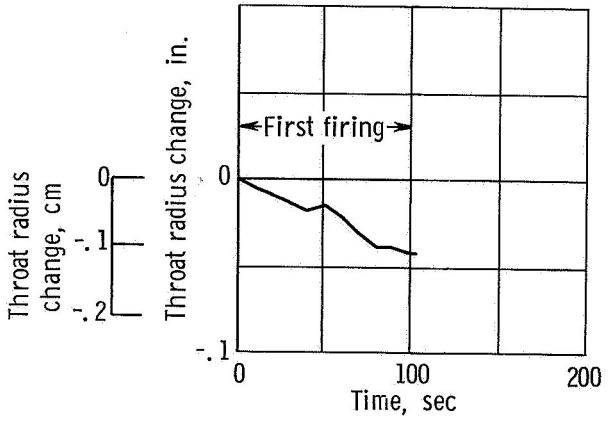

(b) Throat erosion.

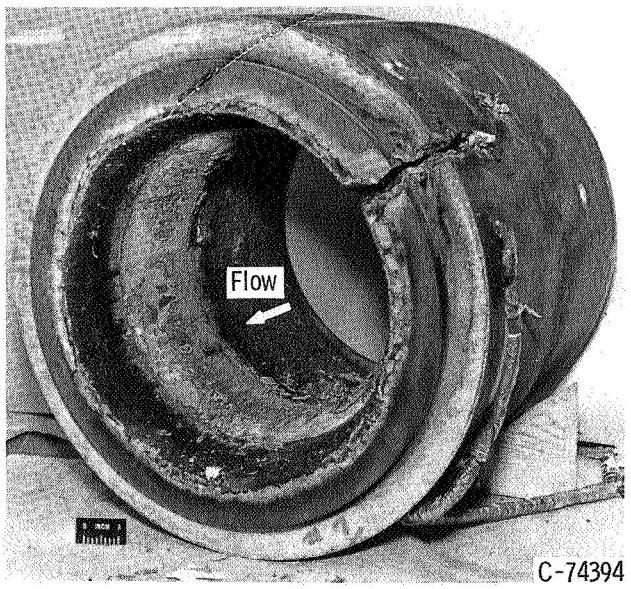

(c) Post-test photograph.

Figure 12. - Profile of insert 3. (All dimensions not otherwise noted are in inches (cm).)

Theoretical analysis predicted no insert stress failure and none occurred. Theoretical analysis also predicted ablative stress failure if no clearance existed between the insert and the ablative material. The most likely cause of ablative cracking was the inadvertent failure during machining to meet the design clearance of 0.015 inch (0.0381 cm) between the zirconia and the ablative envelope.

Insert 3: thin-wall silver-impregnated tungsten. - Figure 13(a) shows the design of insert 3a. The tungsten-silver insert 3, already tested for 102 seconds, was machined to the dimensions of figure 13(a). Ribs were so machined in the ablative envelope that the insert could expand during firing and crush the ribs without cracking the ablative envelope. A steel shell was added to the outside of the ablative envelope to help prevent cracking of the ablative material. The modified insert design was also lighter in weight to simulate more closely a flight-type engine. The modified design decreased the calculated thermal stress in the insert from 66 000 psi (455 MN/sq m) for insert 3 to 46 000 psi (317 MN/sq m) for insert 3a, which gave the modified design a calculated safety factor of 1.5 compared with 1.06 for the original design.

The first firing of insert 3a ended after 17 seconds because of high-frequency combustion oscillations. The second firing ended after 2 seconds because of low chamber pressure. The third and fourth firings both ended after 4 seconds because of high-frequency combustion instability. The first four firings caused two axial cracks completely through the insert about 180° apart. No measurable erosion had occurred (fig. 13(b)). The fifth firing ended after 127 seconds because of combustion oscillations and resulted in a throat erosion of 0.042 inch (0.1065 cm). Figure 13(c) shows the condition of the insert after a total firing time of 256 seconds in two configurations. The chartreuse streaks are tungsten trioxide with significant material loss occurring mainly in the streaks. Since cracking of the insert would have allowed ablative burn-through, testing was ended.

The throat erosion measured for the last 127-second firing of insert 3a was only 0.0003 inch (0.00076 cm) per second compared with an overall rate of 0.001 inch (0.0025 cm) per second in the small-scale tests of reference 2. The erosion due to oxidation in the chartreuse streaks of insert 3a was similar to the erosion over the entire surface of the small-scale insert. The reasons for the differences in behavior for the two sizes are the same as those listed under insert 3. The depletion of silver infiltrant during the firing of insert 3 probably allowed erosion to begin sooner during the testing of insert 3a. The combination of crushable ribs and a steel shell on the outside prevented ablative cracking, but the insert cracked as a result of thermal stress cycling. For applications where many short firings are required, further reduction in thermal stress is necessary. Criteria for thermal stress failure in a cycling environment are different from the simple ultimate stress value used here. A discussion of these effects is given in reference 7.

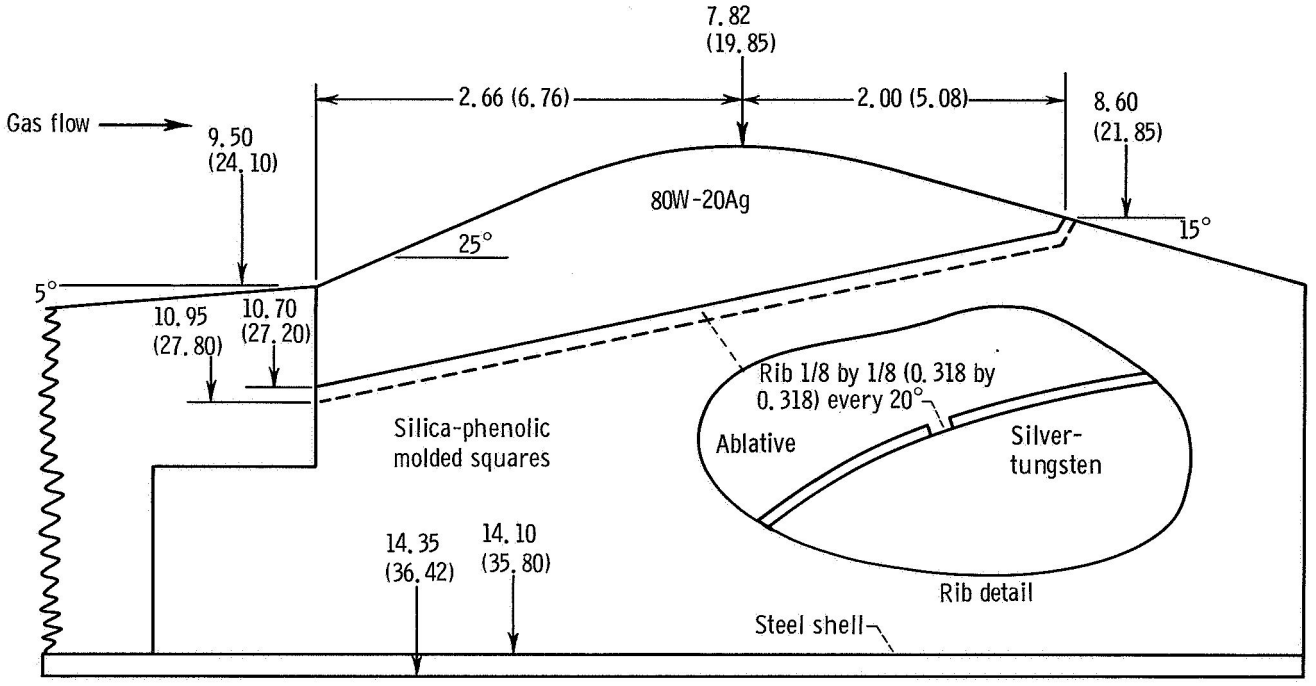

(a) Insert sketch.

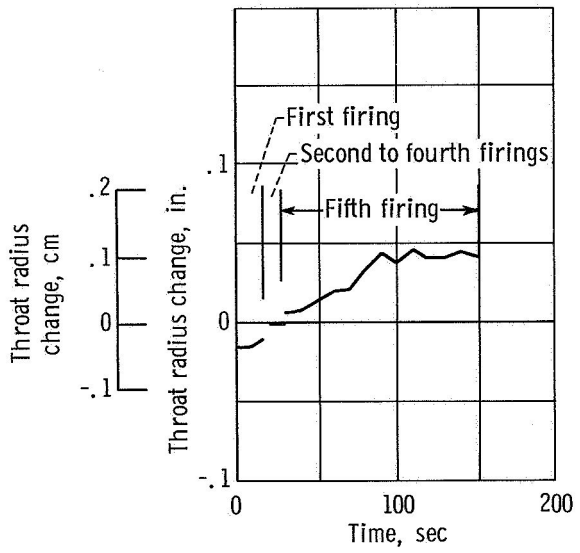

(b) Throat erosion.

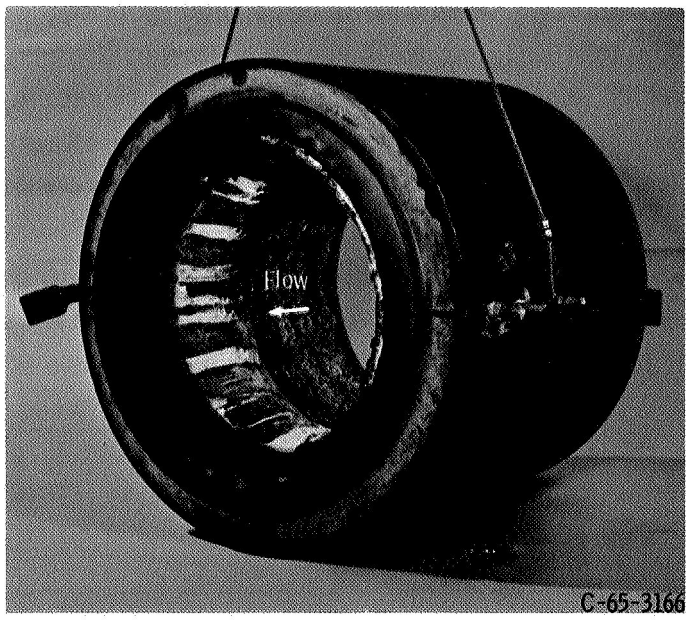

(c) Post-test photograph.

Figure 13. - Profile of insert 3a. (All dimensions not otherwise noted are in inches (cm).)

Insert 4: thick-wall copper-impregnated tungsten. - The design of insert 4 (fig. 14(a)) was the same as the design of insert 3. The nozzles were assembled at the same time. Lack of clearance between the insert and the ablative material caused ablative cracking during testing of insert 3. To prevent ablative cracking around insert 4, a steel split shell was added, as shown in figures 14(a) and (c). The calculated maximum thermal stress in the insert was 66 000 psi (455 MN/sq m) tension, which resulted in a safety factor of 1.67 because of the higher ultimate strength of the tungsten-copper.

The first firing of insert 4 ended at 111 seconds because of a propellant tank capacity limitation. A throat radius increase of 0.012 inch (0.0317 cm) resulted (fig. 14(b)). Cracking of the ablative envelope at the seam in the split shell is visible in figure 14(c). The insert could not be tested further because of combustion gas leakage from the crack in the ablative envelope.

Metallographic analysis detected silicon dioxide and traces of tungsten trioxide on the surface of the insert (fig. 14(c)). Adequate clearance was not provided between the insert and the ablative envelope to allow for differential thermal expansion, and the strength of the steel split shell was not sufficient to keep the ablative material from cracking during firing. The flanges on the split shell yielded sufficiently to allow the crack shown in figure 14(c).

Results for tungsten-copper presented in reference 2 show erosion due to oxidation during one 60-second firing. The throat erosion rate was 0.0003 inch (0.00079 cm) per second compared with 0.0001 inch (0.00025 cm) per second for the large-size insert 4. Possible reasons for lower erosion of the large-size insert are a larger heat-sink capacity leading to a lower surface temperature, a lower oxidizing potential in the large-size combustion environment, or more effective use of the copper infiltrant in the large-size insert, as explained for the silver-infiltrated tungsten.

Theoretical analysis predicted no insert stress failure and none occurred. The ablative envelope cracked because of a lack of adequate clearance for differential thermal expansion between the insert and the ablative envelope. The steel split shell was insufficient to prevent ablative cracking because of the bolt-flange design.

Insert 4a: thin-wall copper-impregnated tungsten. - Figure 15(a) shows the design of insert 4a. The tungsten-copper insert 4, already tested for 111 seconds, was machined to the dimensions of figure 15(a). Ribs were machined in the ablative envelope so that the insert could expand during firing and crush the ribs without cracking the ablative envelope. A steel shell was added to the outside of the ablative envelope also to help prevent cracking of the ablative material. The modified insert design was lighter in weight to simulate more closely a flight-type engine. The modified design decreased the calculated maximum thermal stress in the insert from 66 000 psi (455 MN/sq m) for insert 4 to 46 000 psi (317 MN/sq m) for insert 4a, which gave a calculated safety factor of 2.4 compared with 1.67 for the original design. The first firing of insert 4a ended

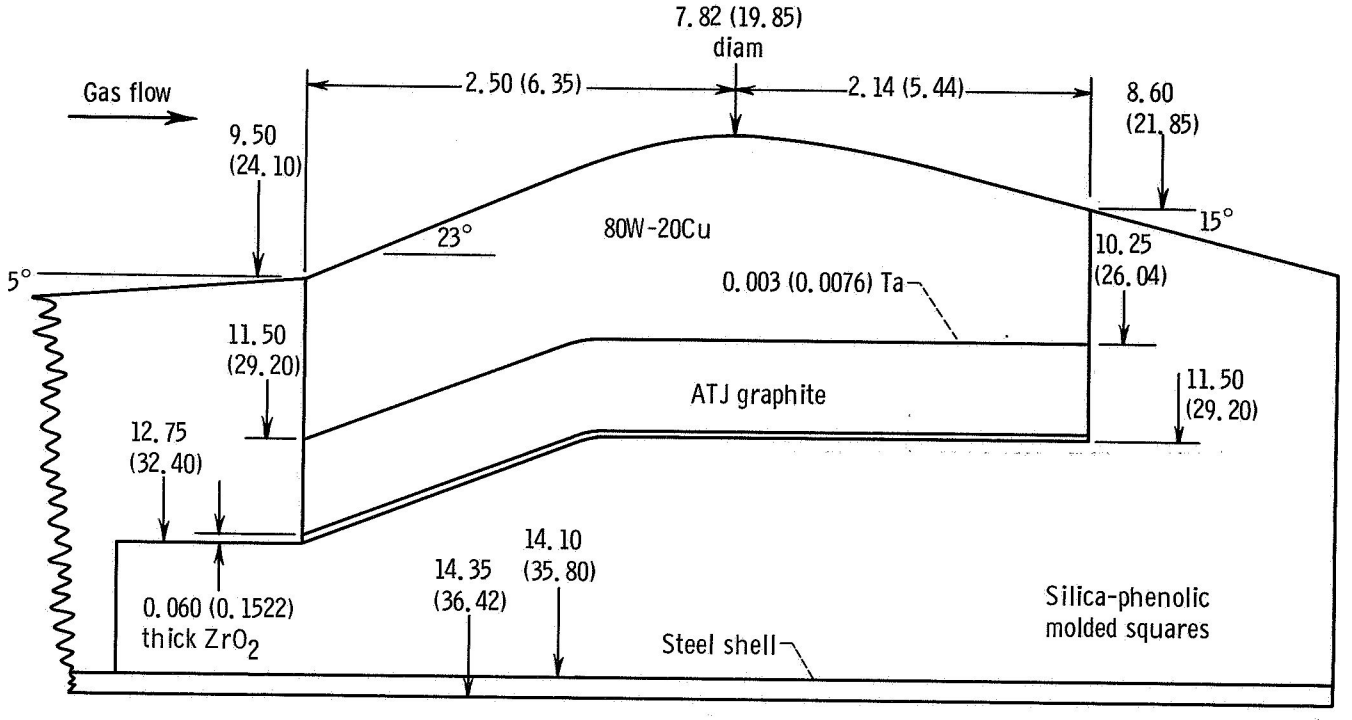

(a) Insert sketch.

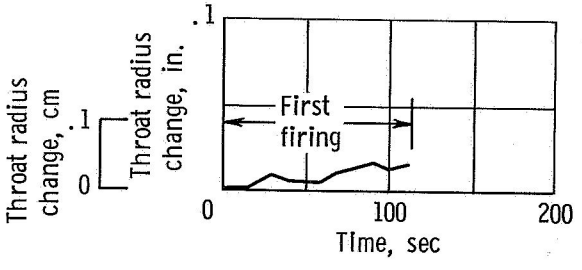

(b) Throat erosion.

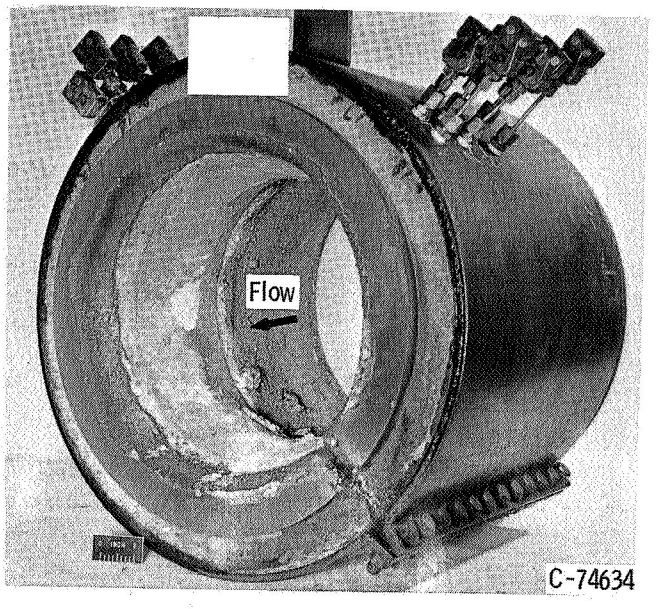

(c) Post-test photograph.

Figure 14. - Profile of insert 4. (All dimension not otherwise noted are in inches (cm).)

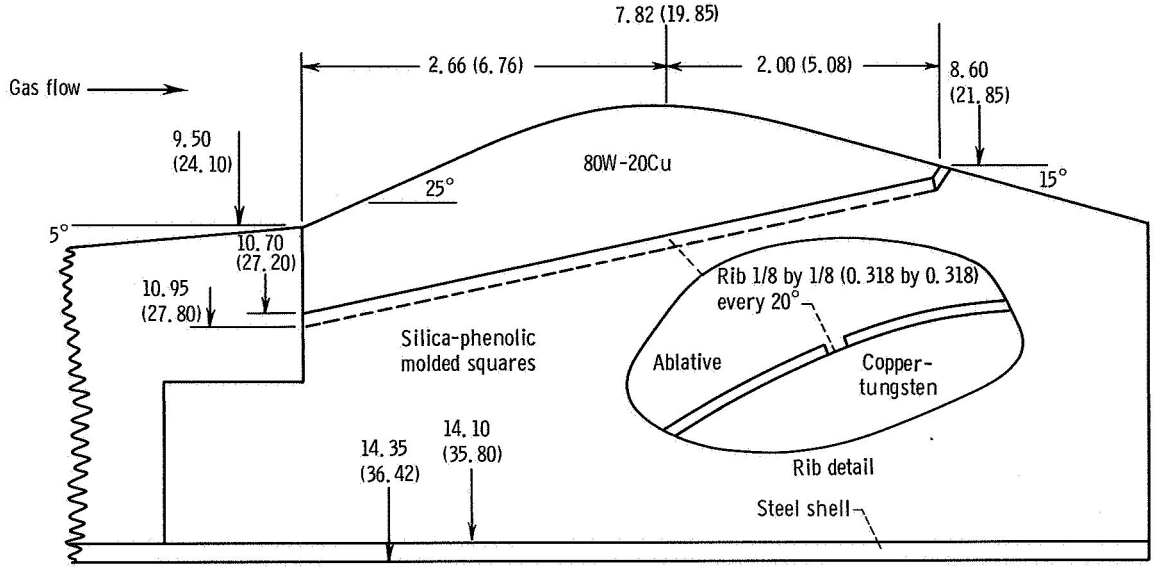

(a) Insert sketch.

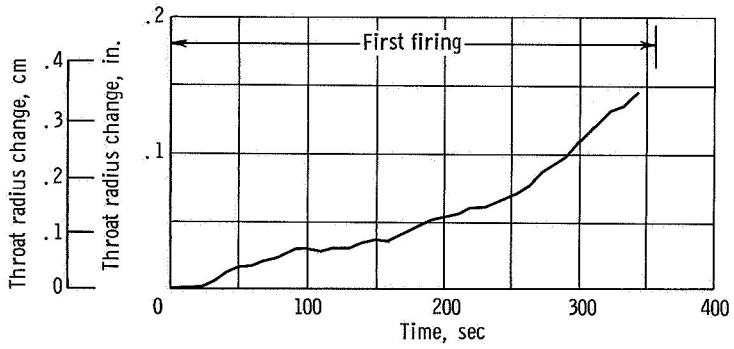

(b) Throat erosion.

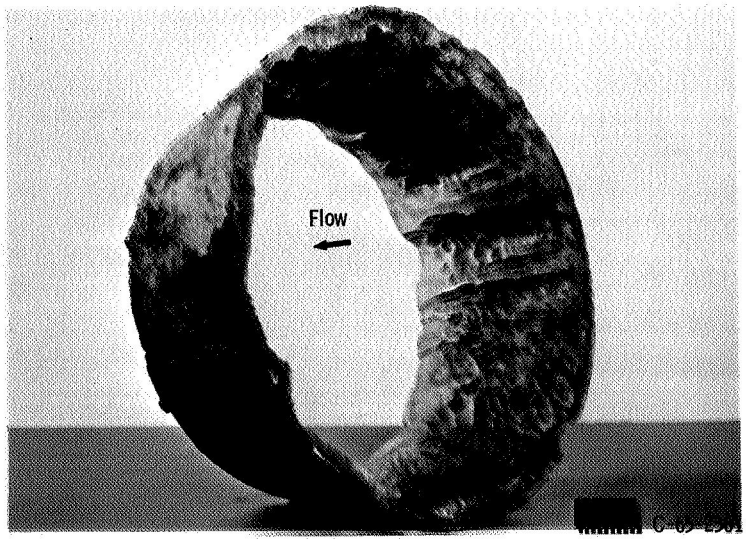

(c) Post-test photograph.

Figure 15. - Profile of insert 4a. (All dimensions not otherwise noted are in inches (cm).)

after 340 seconds because of propellant supply exhaustion of the enlarged propellant tanks. No cracking was evident. Continuous throat erosion during the test is shown in figure 15(b). The change in slope could have been caused by copper depletion near the surface of the insert. Post-test chemical analysis revealed very little copper present on the surface. Despite the craterlike appearance shown in figure 15(c), the erosion of insert 4a was due to oxidation and not to spalling (see film supplement). The leading edge (0.600 in. or 1.52 cm thick) of the insert is completely exposed. This exposure shows that ablative material erosion in this area was at least 0.600 inch (1.52 cm) during the 340-second firing. Disassembly of the insert showed that some of the combustion gases had been flowing around the outside of the insert. The flow probably began late in the firing after the leading edge of the insert was exposed. The failure mode (oxidation) of insert 4a was the same as the failure in the small-scale testing of reference 2. The erosion rate was 0.0008 inch (0.002 cm) per second for the small-scale test compared with 0.0004 inch (0.001 cm) per second for the large-scale test. The increased erosion resistance for the large-scale inserts could have been due to a larger heat-sink capacity, a less oxidizing environment, or more effective use of the infiltrant copper. Depletion of the copper infiltrant during the firing of insert 4 probably allowed erosion to begin sooner during the firing of insert 4a.

The theoretical analysis predicted no insert stress failure and none occurred. The combination of crushable ribs in the ablative material and a steel shell on the outside of the ablative material prevented cracking of the ablative envelope.

Summary. - Copper- and silver-infiltrated tungsten gave similar erosion resistance. For the first 100 seconds, negligible erosion was measured for the large heat-sink design. A rate of 0.0003 to 0.0004 inch (0.00076 to 0.001 cm) per second was measured during subsequent firings. This rate compares with a standard ablative erosion of 0.0004 inch (0.001 cm) per second during the first 100 seconds and 0.0015 inch (0.0038 cm) per second during the next 150 seconds (ref. 1). Ablative erosion rates were obtained with the same injectors used to test these inserts.

The tungsten-copper combination did not crack and generally gave higher calculated safety factors than tungsten-silver.

The crushable ribs and steel-shell combination prevented cracking of the ablative from differential thermal expansion as experienced in the initial insert assembly.

Ablative erosion at the insert leading edge allowed gas leakage around the outside of the insert. The insert must be extended to a chamber diameter (lower velocity region) where ablative erosion is less severe to solve this problem.

Pyrolytic Graphite Coatings

Insert 5: 0.050-inch (0.127-cm) pyrolytic graphite on carburized substrate. - A primary disadvantage often experienced with coatings of pyrolytic graphite on conven-

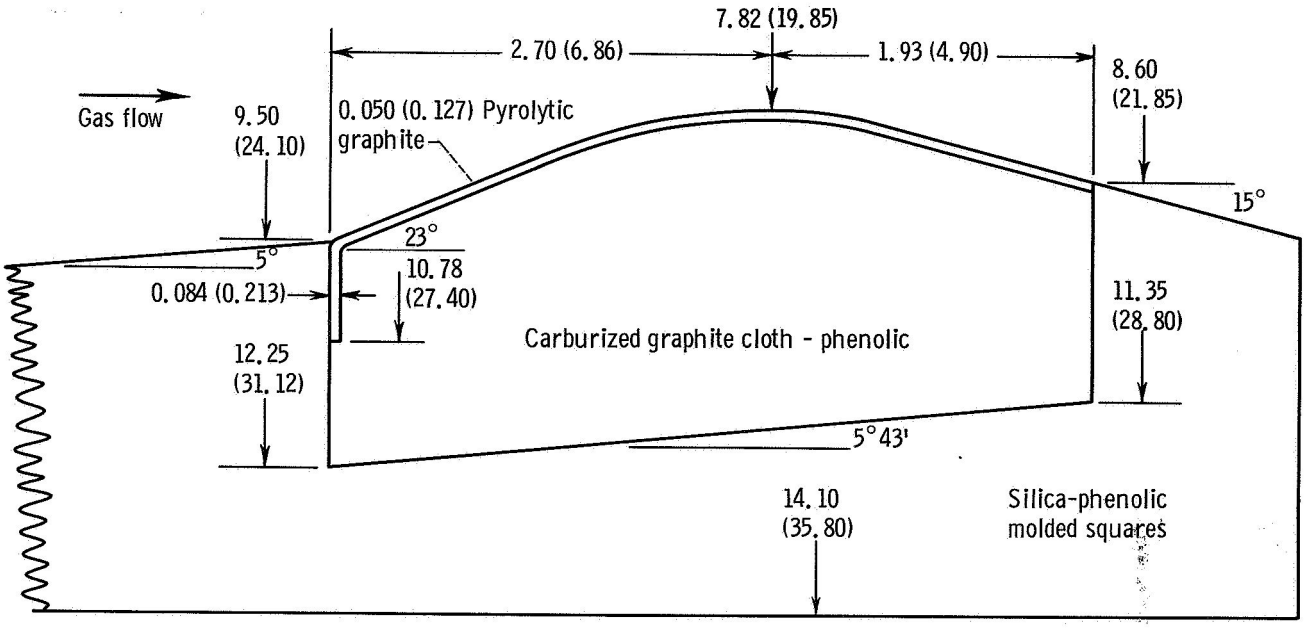

(a) Insert sketch.

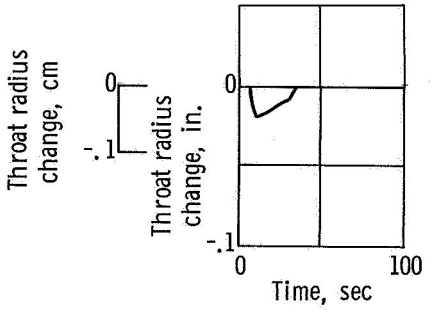

(b) Throat erosion.

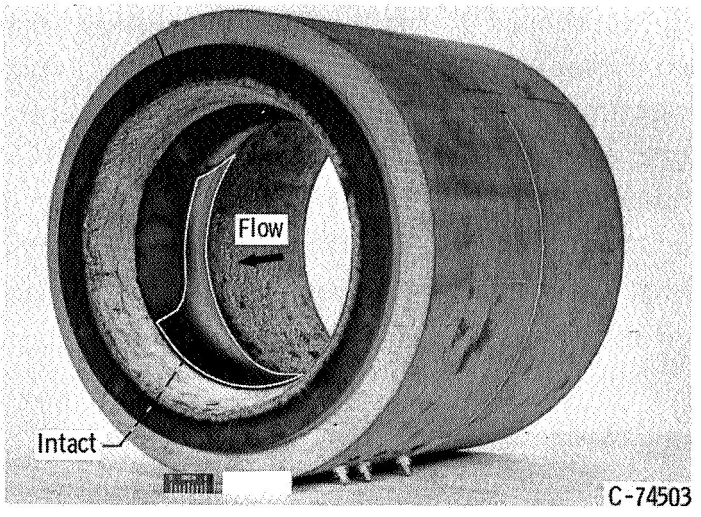

(c) Post-test photograph.

Figure 16. - Profile of insert 5. (All dimensions not otherwise noted are in inches (cm).)

tional types of graphite substrates is the loss of the coating by delaminations, cracking, or loss of coating adhesion. To adequately assess the quantitative potential of a coating to resist the oxidation and thermal erosion environment, it is necessary first to ensure the structural compatibility of the coating with its substrate. The substrate employed in insert 5 was specifically designed to maximize the coating-substrate compatibility. A 25-percent phenolic resin substrate, reinforced with graphite cloth, was subjected to a slow carburizing process. This process was followed by pyrolysis at approximately 2000° F (1366° K) in a nitrogen gas environment to partial graphitization. The substrate thus produced, when related to conventional graphites, was (1) more isotropic, (2) semiporous for maximum coating diffusion with subsequent increased adhesion, (3) of lower modulus of elasticity, and (4) lighter in weight. The 0.050-inch (0.127-cm) pyrolytic graphite coating was applied by a conventional vapor deposition process. To minimize the distance from the leading edge to the throat, an entrance diameter of 9.50 inches (24.1 cm) was chosen (see fig. 15(a) for details).

Running of insert 5 was terminated at the first sign of coating failure at the throat after about 30 seconds (fig. 16(b)). The failure mechanism was a delamination of the pyrolytic graphite layer planes. It was felt that this delamination was caused primarily by the residual stresses produced during the heating and cool-down cycles during the deposition process. The relatively high Mach number of the combustion gases at the insert leading edge may have contributed to initial coating removal in this area. The postfiring photograph (fig. 16(c)) shows areas in the throat with the coating missing and corresponding areas upstream with the coating also missing. The reverse is true for those areas where the coating at the throat remains intact.

Coating adhesion to the same substrate in the small-scale tests was adequate, and failure occurred because of oxidation and not delamination of layer planes. The firing of insert 5 suggests that, in addition to proper substrate material properties, other means must be found to ensure coating substrate compatibility. It was impossible to analyze for residual stresses inherent in the deposition process, and no correlation with the firing results can be made.

Insert 6: 0.100-inch (0.254-cm) pyrolytic graphite on carburized substrate. - The same type substrate was used for insert 6 as for insert 5. Two design changes were made: The insert leading edge was extended to the chamber diameter, and the coating thickness was increased to 0.100 inch (0.254 cm) (see fig. 17(a)).

The insert survived for approximately 70 seconds before a large increase in the throat radius was recorded (fig. 17(b)). As with insert 5, the primary failure mode was layer plane delaminations, probably caused by residual stresses within the coating. Most of the material loss was in the throat region with most of the coating still intact upstream (fig. 17(c)). The area of severe vulnerability would appear to be the tangency point where the entrance half-angle and the throat radius of curvature meet.

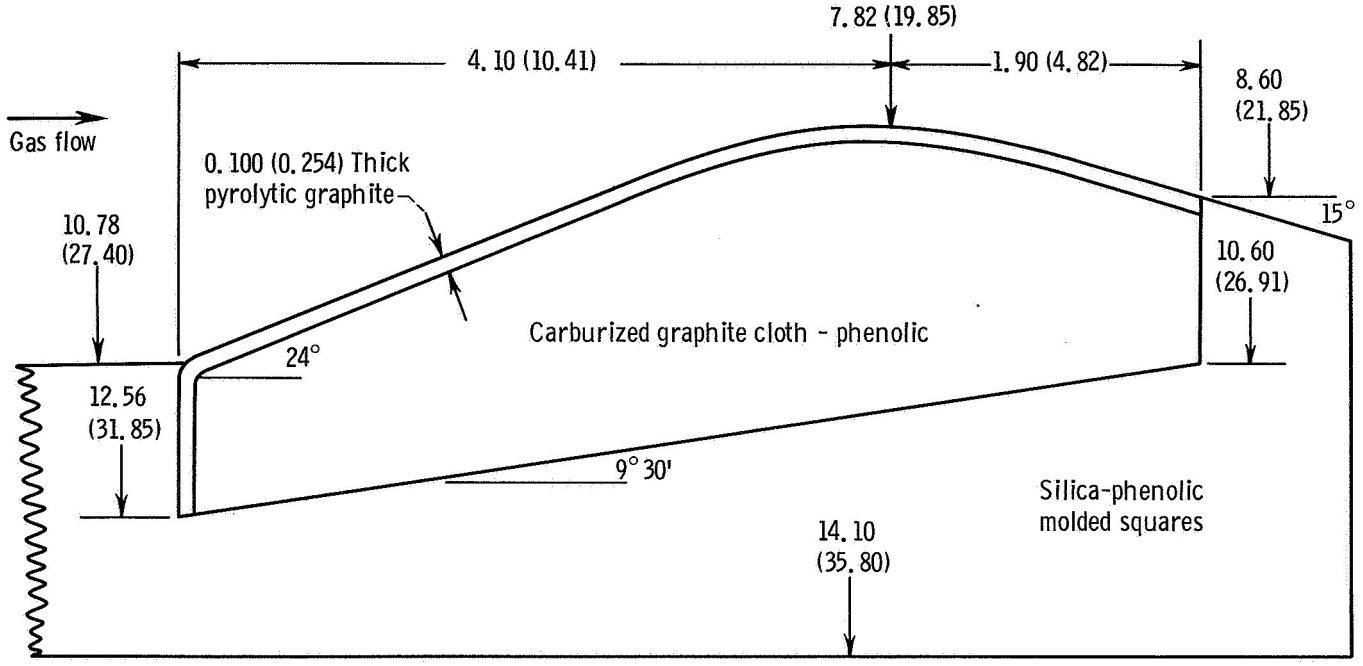

(a) Insert sketch.

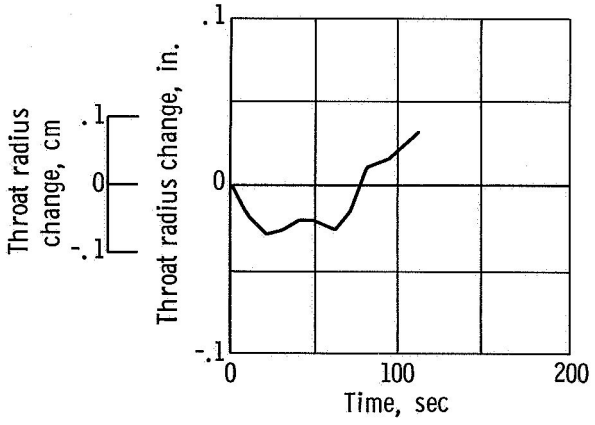

(b) Throat erosion.

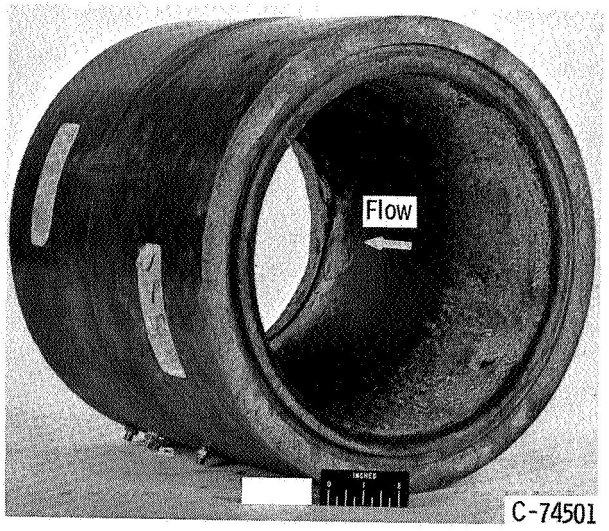

(c) Post-test photograph.

Figure 17. - Profile of insert 6. (All dimensions not otherwise noted are in inches (cm).)

None of the small-scale inserts coated with pyrolytic graphite failed structurally at the tangency point of nozzle curvature. This effect appears more critical in larger-size nozzles with relatively thick coatings (0.100 in. or 0.254 cm). Small-scale inserts with coatings ranging from 0.010 to 0.060 inch (0.0254 to 0.152 cm) thick generally failed within 60 seconds. The failure mode was oxidation or loss of adhesion or both, beginning at the insert leading edge and progressing to the throat plane.

Insert 7: 0.010 inch (0.0254 cm) pyrolytic graphite coating, heat treated. - The substrate used for insert 7 was obtained by machining the residual coating from the inside diameter of insert 5. Two design changes were made in an attempt to eliminate the delamination problem. The coating thickness was reduced to 0.010 inch (0.0254 cm) and during the deposition process the insert was subjected to an annealing process to remove residual stresses. (See fig. 18(a) for the final design.)

The insert was fired initially for 47 seconds when high-frequency instability was detected and the run aborted. Examination of the insert showed minor cracking and some coating loss upstream of the throat. The remainder of the coating looked good and well bonded to the substrate, and a second run was made. The insert was fired for an additional 80 seconds prior to detectable throat erosion. The shape of the erosion curve (fig. 18(b)) together with the appearance of the fired insert (fig. 18(c)) is indicative of an oxidation failure rather than delamination of cracking. The erosion of this thin-wall coating is of the same order of magnitude as was determined in the small-scale testing (no throat erosion after approximately 60 sec) in which oxidation was given as the primary failure mode.

Insert 8: 0.010-inch (0.0254-cm) pyrolytic graphite on PT 0178 graphite. - The substrate used for insert 8 was a commercial grade of graphite with properties very similar to the special substrate material used on inserts 5 to 7. It is described as National Carbon grade PT 0178. It was considered desirable to find a commercial grade of graphite which exhibited properties beneficial to coating retention rather than to use a specially prepared substrate. A 0.010-inch (0.0254-cm) coating was chosen to minimize delamination and cracking. Figure 19(a) shows the nozzle design. The test firing was stopped when a significant increase in the throat radius was detected, about 60 seconds into the run (fig. 19(b)). The rapid throat radius change and the post-test photograph together with the film supplement (fig. 19(c)) indicate a loss of coating due to a combination of delamination and cracking. The substrate erosion rate was similar to the erosion rate of the previously used substrate. A greater degree of surface porosity was apparent on this substrate.

Insert 9: 0.010-inch (0.0254-cm) pyrolytic graphite and boron (heat-treated) coatings on PT 0178 substrate. - Insert 8 was machined to remove residual coating from the inside diameter and recoated to form insert 9. In an attempt to eliminate the delamination and cracking problem, a 0.010-inch (0.0254-cm) coating was applied with the same

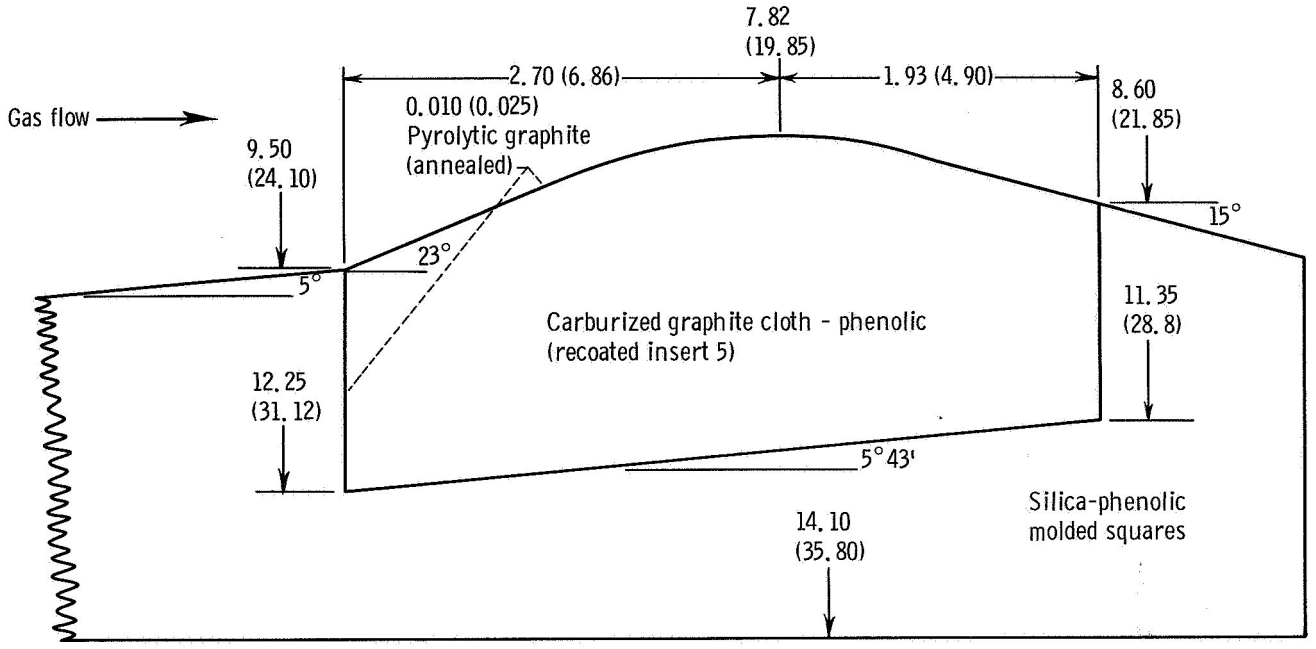

(a) Insert sketch.

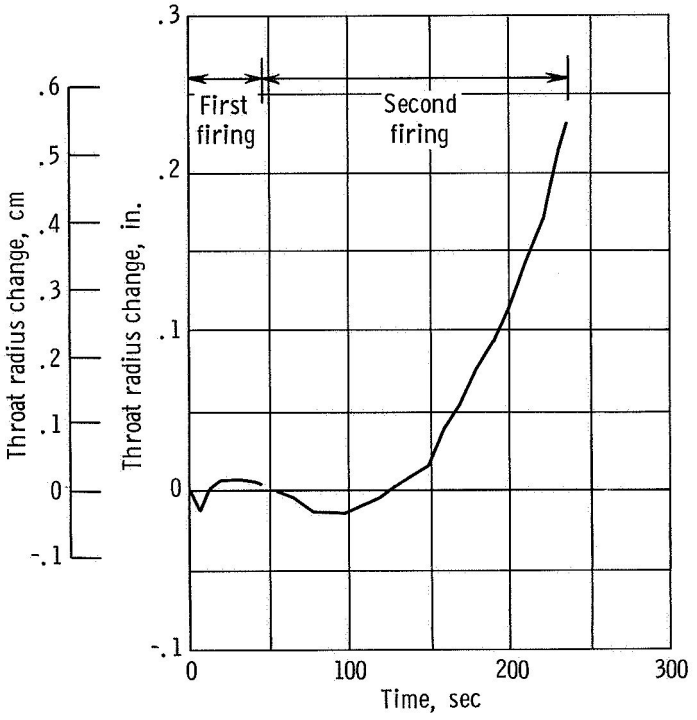

(b) Throat erosion.

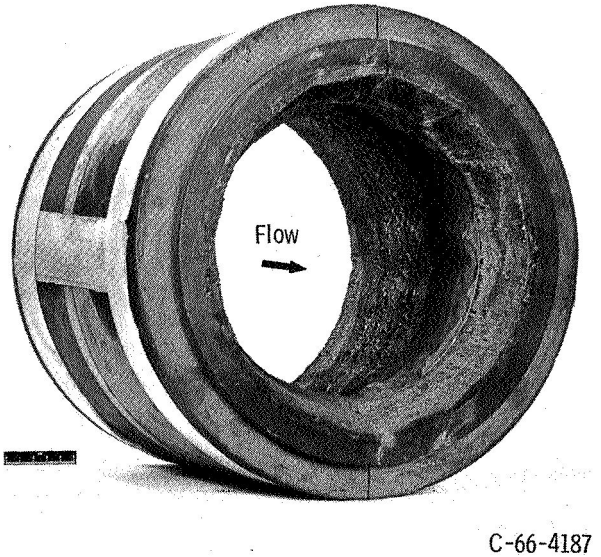

C-66-4187

(c) Post-test photograph.

Figure 18. - Profile of insert 7. (All dimensions not otherwise noted are in inches (cm).)

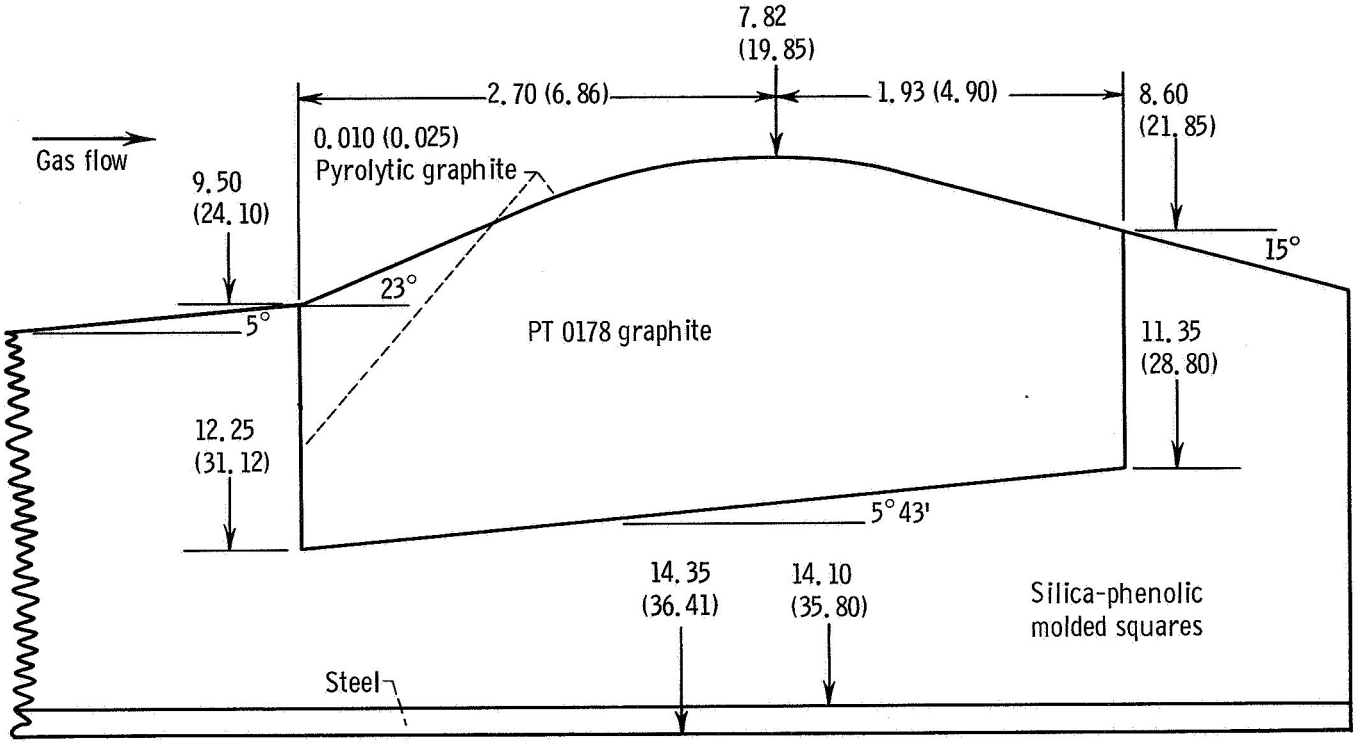

(a) Insert sketch.

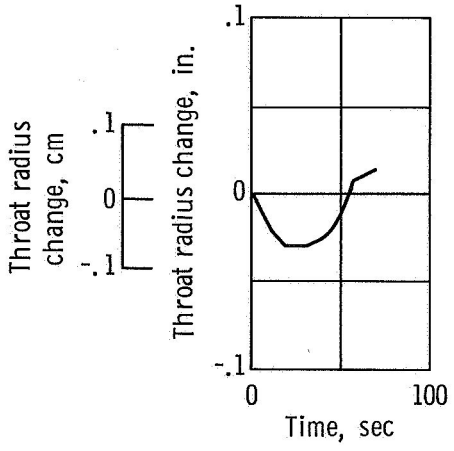

(b) Throat erosion.

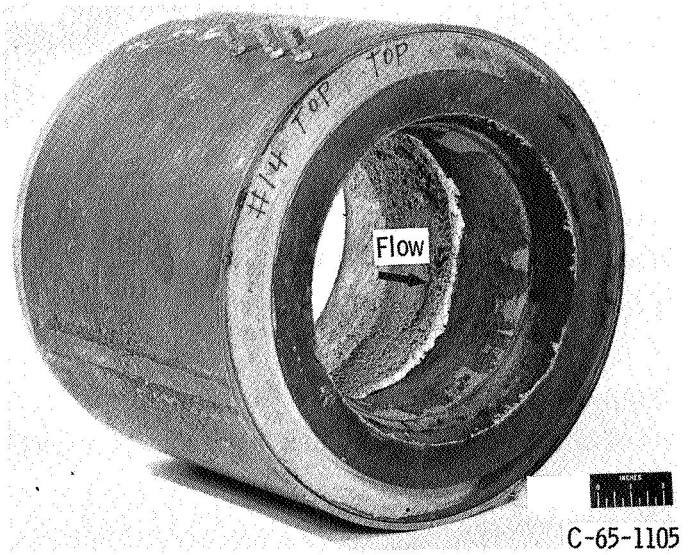

(c) Post-test photograph.

Figure 19. - Profile of insert 8. (All dimensions not otherwise noted are in inches (cm).)

annealing and heat-treating process which seemed successful for insert 7. A codeposit of boron with the pyrolytic graphite was used to increase the oxidation resistance of the coating. The concentration of boron was approximately 0.5 percent by weight. The nozzle design is shown in figure 20(a).

Insert 9 was fired for 150 seconds continuously before any significant throat radius change was noted (fig. 20(b)). The last 20 seconds prior to shutdown resulted in rapid substrate erosion. The post-test photograph (fig. 20(c)) shows much of the coating still intact downstream of the throat together with a large axial crack in the substrate. Apparently, the insert maintained its integrity for about 140 seconds, at which time the coating was probably lost, primarily because of oxidation. After loss of the coating, the substrate failed by thermal stress and rapid erosion. The same coating was not used in small-scale tests, however. The failure mode for a similar coating (progression from the leading edge) was the same as in the small-scale tests, but the time was extended from 60 seconds in the small-scale to 150 seconds in the large-scale tests.

Although a mathematical calculation was impossible, a degree of correlation may be made between the results achieved and the expected results. On the basis of previous firing experience and a qualitative knowledge of material behavior in the rocket engine combustion environment, it was concluded that the oxidation resistance of pyrolytic graphite must be improved. Apparently, the addition of boron was successful in increasing the resistance of the coating to oxidation.

Summary. - The area of maximum stress appears to have occurred at the tangency point of the entrance convergent angle and the insert throat radius of curvature. To relieve this stress, a thin coating on a low-modulus, high-expansion substrate (to match the high expansion of the coating) was tried. Adhesion of the coating to the substrate was most successful when heat-treating or annealing was employed during the deposition process. The oxidation resistance of the coating was appreciably increased when boron was codeposited along with the pyrolytic graphite. Although manufacturing techniques will have to be modified, it may be desirable to increase the boron content and hopefully to increase the oxidation resistance still further. The heat-treating process was necessary to relieve the stresses encountered during the coating process and maintain coating adhesion during the extended firing duration.

Silicon Carbide Coatings

Insert 10: 0.040-inch (0.1015-cm) pyrolytic silicon carbide on graphite. - Insert 10 was a pyrolytic deposition of silicon carbide on a high-modulus graphite substrate. The substrate used for insert 10 was chosen to match the thermal expansion of the silicon carbide coating. The same type of coating had been successful on small reaction control

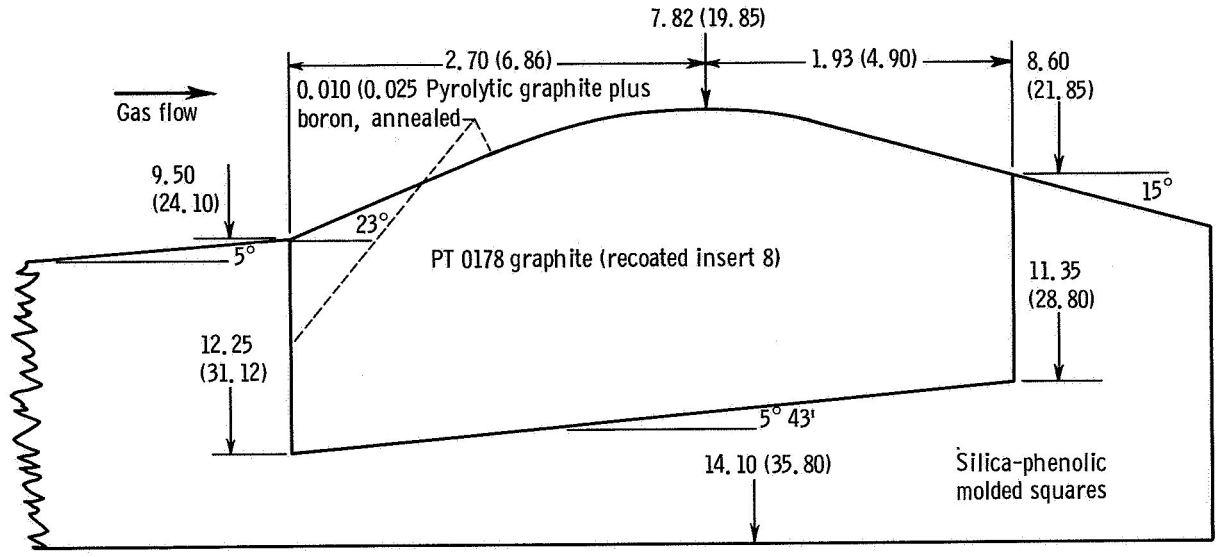

(a) Insert sketch.

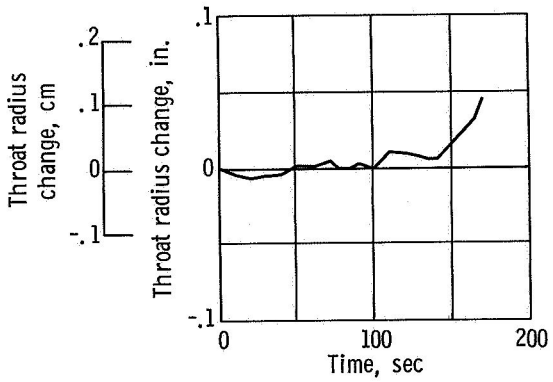

(b) Throat erosion.

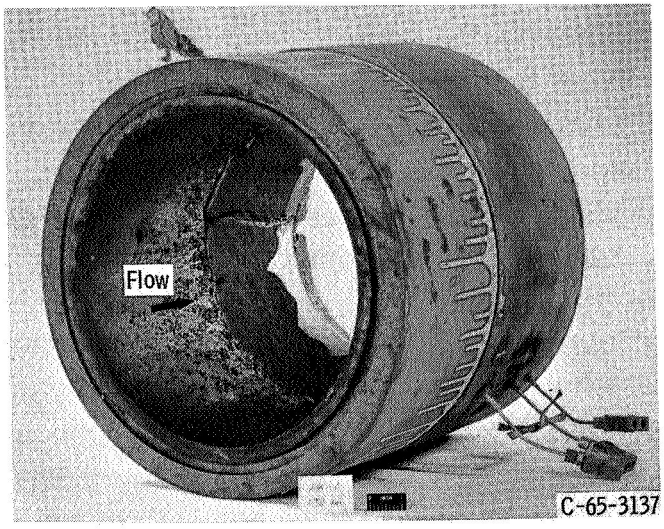

(c) Post-test photograph.

Figure 20. - Profile of insert 9. (All dimensions not otherwise noted are in inches (cm).)

engines (ref. 2). An evaluation of the applicability for larger-size engines in the design of figure 21(a) was needed.

The insert test was run for a total of 105 seconds, although the coating failed in the first few seconds of the run (fig. 21(b)). The film of this test clearly shows the coating cracking and leaving the surface of the substrate prior to 10 seconds of testing.

A chemical analysis of the remaining coating detected a thin layer of silicon dioxide either from coating oxidation or the ablative material upstream. The primary failure was structural because of thermal stress, and the remaining coating was scaly and loosely bonded to the substrate (fig. 21(c)). An accurate assessment of the oxidation resistance of the pyrolytic silicon carbide in large scale cannot be made until the structural problem is solved. The same coating was tested in a 1.2-inch- (3.04-cm) diameter throat insert (ref. 2). The insert survived four firings totaling 722 seconds in duration before failure. The failure mode in small-scale tests was oxidation after approximately 250 seconds of continuous firing, while the larger-scale insert failed structurally.

Insert 11: 0.005-inch (0.0127-cm) silicon carbide - pack cementation (diffusion coating). - The substrate of insert 11 was selected to improve adhesion and thermal shock resistance and to match more closely the thermal expansion of the silicon carbide coating. The low-modulus, high-expansion, porous PT 0178 was used as the substrate material. In place of pyrolytic deposition, the silicon carbide was applied by diffusion with the use of the pack cementation process. The depth of penetration was approximately 0.100 inch (0.254 cm), and the surface layer of silicon carbide was approximately 0.005 inch (0.0127 cm). Figure 22(a) details the design.

The insert was tested for approximately 70 seconds before the start of rapid erosion. The inner layer (0.005 in. or 0.0127 cm) was assumed to be gone at this time. The firing was continued for a total of 210 seconds to assess the erosion rate of the diffusion layer and the PT 0178 substrate (fig. 22(b)). The rate for the first 100 mils (0.254 cm) erosion was somewhat lower than for the remainder of the run (0.0022 in./sec or 0.0056 cm/sec compared with 0.003 in./sec or 0.0076 cm/sec), which would indicate superior erosion resistance for the silicon carbide - graphite material.

A pretest examination of the diffusion coating indicated lack of continuity in the silicon carbide. At many discrete sites the substrate was exposed. The actual effect of the diffusion coating was to present a silicon carbide - graphite matrix to the gas stream. The first 0.005 inch (0.0127 cm) of thickness was predominently silicon carbide and the next 0.100 inch (0.254 cm) was predominantly graphite. During the first 70 seconds of testing, erosion apparently due to oxidation removed the layer which was mostly silicon carbide. During the next 50 seconds, the graphite - silicon carbide was removed by oxidation at a rate of 0.0022 inch (0.0056 cm) per second. For the remainder of the test, the porous graphite substrate was removed by oxidation at a rate of 0.003 inch

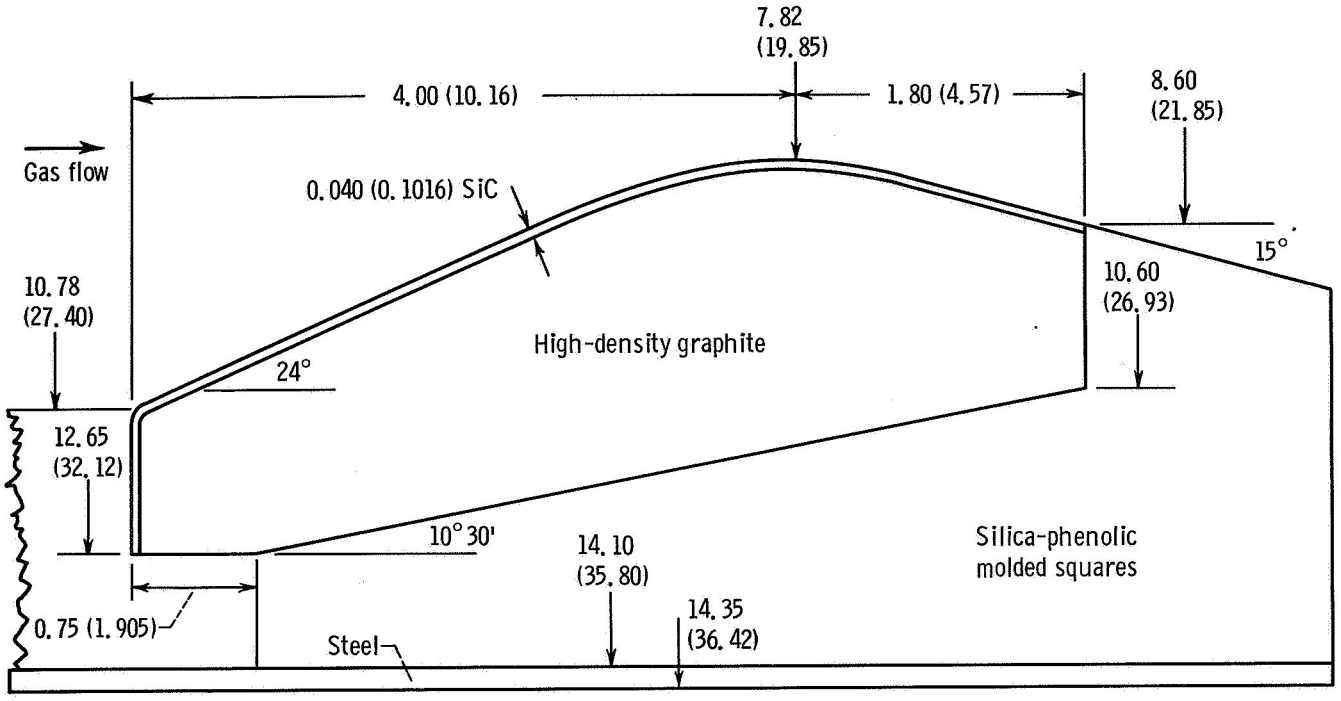

(a) Insert sketch.

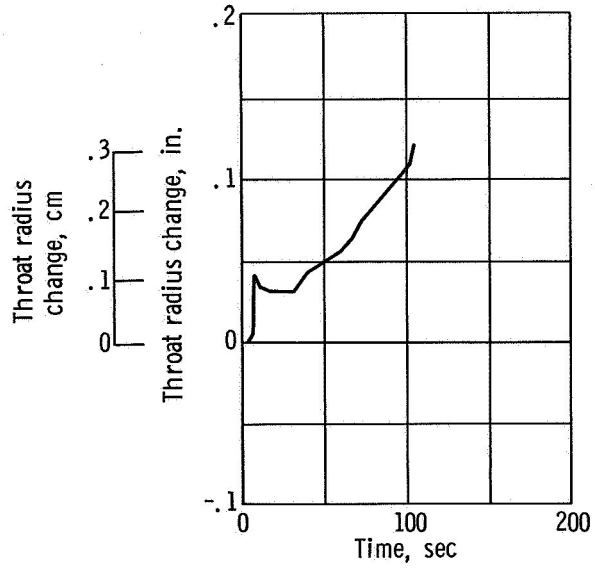

(b) Throat erosion.

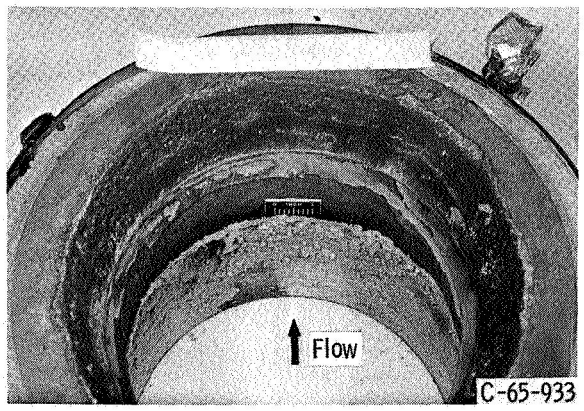

(c) Post-test photograph.

Figure 21. - Profile of insert 10. (All dimensions not otherwise noted are in inches (cm).)

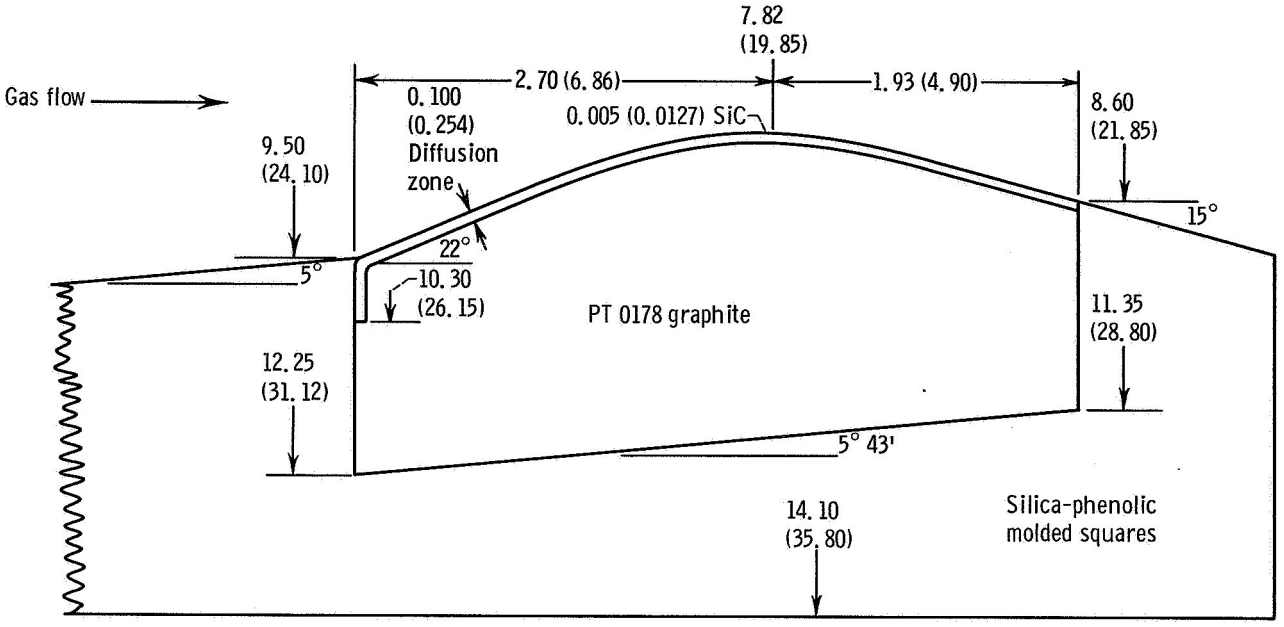

(a) Insert sketch.

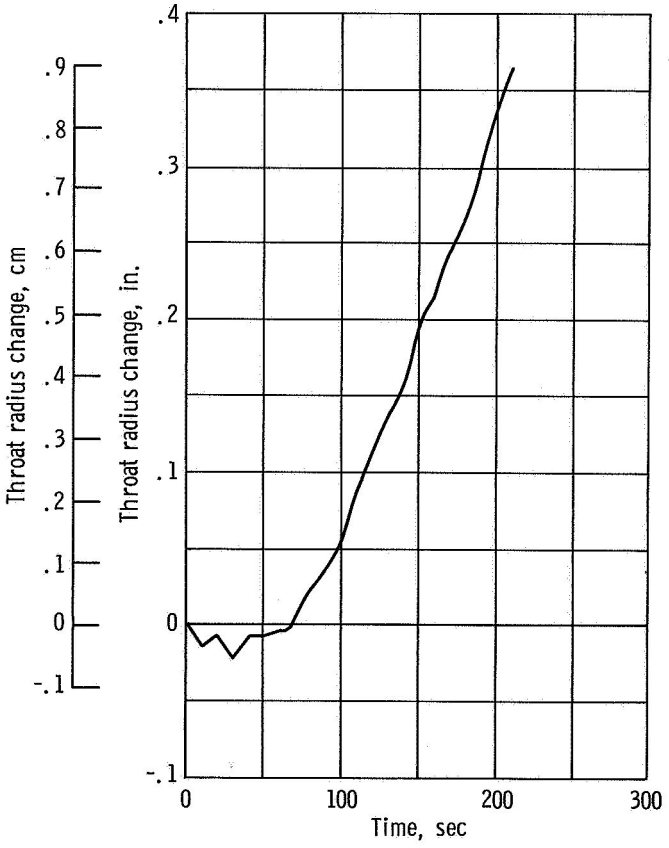

(b) Throat erosion.

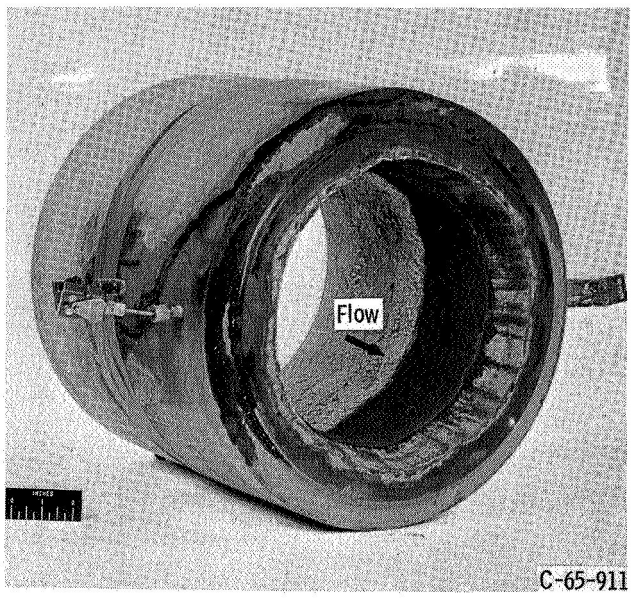

(c) Post-test photograph.

Figure 22. - Profile of insert 11. (All dimensions not otherwise noted are in inches (cm).)

(0.0076 cm) per second. Figure 22(c) shows the condition of the substrate following testing.

The same coating technique was used to make a 1.2-inch- (3.04-cm) throat-diameter insert with a less porous substrate. A 60-second firing removed most of the 0.005-inch- (0.0127-cm) thick layer when silicon carbide predominated. The oxidation attacked the graphite sites preferentially, but the entire surface was oxidized. For the diffusion-coated silicon carbide insert, the failure mode was the same in both sizes.

Summary. - The pyrolytically deposited silicon carbide coating failed by thermal stress. To solve the structural problem, an annealing or heat treatment process might be used, as was done with pyrolytic graphite. Other alternatives include a thinner coating to reduce thermal stress or a different substrate to provide better bonding and thermal expansion characteristics.

The diffusion coating of silicon carbide solved the structural problem but failed by oxidation, partly because of its noncontinuous structure. The thickness of silicon carbide could be increased beyond 0.005 inch (0.0127 cm) until the substrate is completely covered. If this is impossible, a thin pyrolytic deposition could be made over the diffusion coating.

Pyrolytic Graphite

Insert 12: preferentially oriented pyrolytic graphite. - A throat insert was designed to take advantage of the unique properties of pyrolytic graphite. The material is highly conductive in the ab-plane and an insulator in the c-direction. Experience with small-size inserts (ref. 2) showed that orienting the ab-plane radially prevented oxidation of the pyrolytic graphite for 120 seconds but overheated the ablative envelope around the insert which caused loss of the insert. Also, in subscale tests, orienting the ab-plane axially prevented overheating of the ablative material but led to insert failure by delamination of the layer planes. The design shown in figure 23(a) was an attempt to combine the two configurations tested in reference 2. The layer planes in this design were formed by a continuous vapor deposition process which resulted in individual layers approximately 0.100 inch (0.254 cm) thick. A two-piece structure was produced, one piece oriented to conduct heat away from the throat (shaded planes in fig. 23(a)) and the other piece oriented to insulate the ablative material and to conduct excess heat into the nozzle exit cone. The design goal was to maintain the inside surface temperature of the pyrolytic graphite below the oxidation threshhold temperature. The layer planes were also oriented to minimize delamination, but fabrication problems limited the angle at which the planes could be oriented with respect to the gas stream.

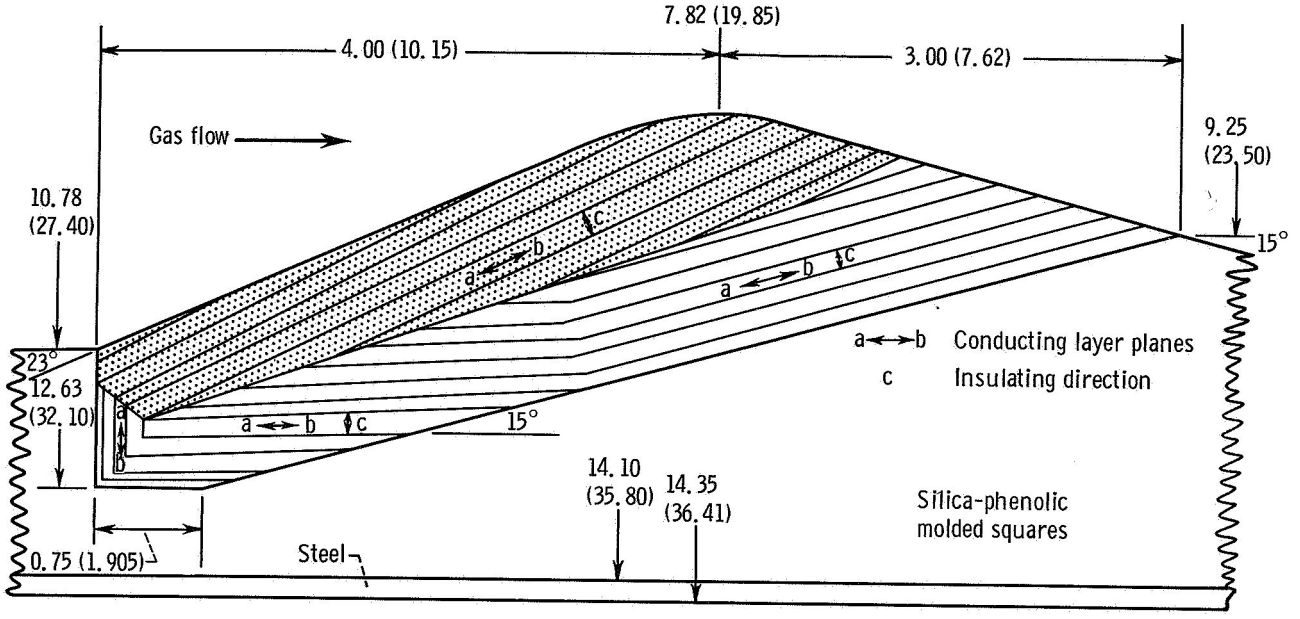

(a) Insert sketch.

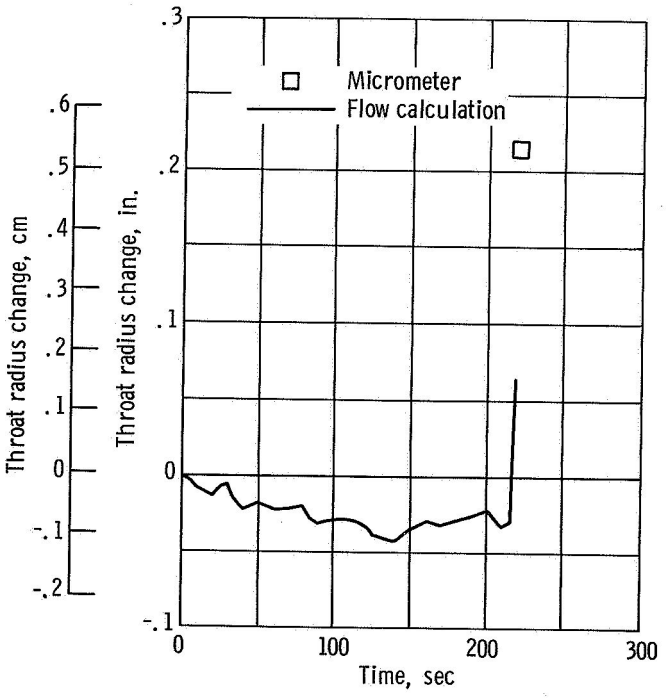

(b) Throat erosion.

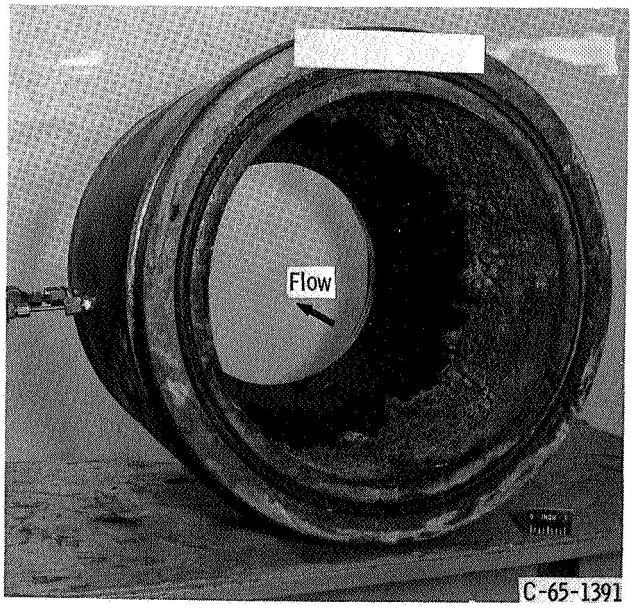

(c) Post-test photograph.

Figure 23. - Profile of insert 12. (All dimensions not otherwise noted are in inches (cm).)

The throat erosion plot of figure 23(b) shows no throat erosion until 218 seconds, when an abrupt radius increase occurred. Testing was ended at this time. A postfiring inspection of the insert revealed that the shaded layer planes of figure 23(a) were missing. Figure 23(c) is a post-test photograph of the insert. Because of the abrupt nature of the failure, it was concluded that delamination was the cause of failure. There was no evidence of oxidation on the exposed layer plane. A large nodule and axial cracks visible in figure 23(c) support the structural failure conclusion. Overheating of the ablative envelope around the insert was not a problem. Therefore, the planes could have been oriented at a higher angle to the centerline if fabrication techniques had been available. This would also have enabled the throat to operate at a lower temperature. The heat flux to the ablative material would have increased, but the delamination failure might have been averted. The condition of the ablative at the insert leading edge (fig. 23(c)) is rough and bubbly without high erosion. The extension of the insert diameter to the full chamber diameter allowed a relatively long-duration firing without the high ablative erosion experienced in other designs.

The large-scale insert gave longer continuous throat erosion resistance than any of the simpler smaller-scale designs. Delamination of the small-scale insert was relatively constant at the rate of 0.0012 inch (0.003 cm) per second. Erosion due to oxidation for the washer configuration was an overall rate of 0.00012 inch (0.0003 cm) per second, but the longest single firing was 126 seconds, which led to loss of the insert due to deterioration of the ablative material around the insert. The large-scale design eliminated overheating of the ablative envelope but not the delamination problem.

CONCLUDING REMARKS

A general conclusion which may be drawn from the results is that throat inserts have the potential to reduce throat erosion and thus increase the performance of ablative thrust chambers. While several inserts demonstrated reasonable durability, further improvements in structural integrity and oxidation resistance are required to provide extended duration capability. The two prime failure mechanisms are discussed in relation to the individual inserts tested. Recommendations to improve reliability are made where possible.

STRUCTURAL INTEGRITY

To ensure reliability and prevent possible catastrophic failure, structural integrity must be maintained.

When the silicon carbide insert cracked, the thrust chamber burned through. This burn-through was caused by loss of pieces of the silicon carbide insert. Although the same type of cracking failure occurred in the 1.2-inch (3.04-cm) throat test, no pieces were lost. Because of the increased stress problems associated with larger-size inserts, the possibility of catastrophic failure is greatly increased. Loss of insert pieces at the leading edge possibly could be prevented by eliminating erosion of the ablative material upstream. An approach section made of JTA graphite would probably be satisfactory at a flow Mach number between 0 and 0.30 and is recommended in all cases where it is not practical to extend the insert material itself to an increased diameter.

Copper-infiltrated tungsten was structurally superior to silver-infiltrated tungsten although the duty cycles were different. Cracking of the ablative envelope in the initial infiltrated tungsten design illustrated the need for careful attention to design detail and assembly techniques.

The pyrolytically deposited graphite and silicon carbide coatings failed by thermal stress. When a 0.010-inch- (0.0254-cm) thick pyrolytic graphite coating was heat-treated to relieve the residual stresses, no structural failure of the coating occurred. Application of heat-treating techniques to thicker coatings could solve the structural problems and also increase the erosion resistance.

The structural failure of the preferentially oriented pyrolytic graphite insert occurred quite suddenly. Orientation of the layer planes at a higher angle to the gas flow and increased interlaminar shear strength might solve this problem.

EROSION RESISTANCE

The erosion resistance of tested inserts is compared with the erosion resistance of ablative nozzles reported in reference 1. Improvements in erosion resistance are noted and recommendations for further improvements are made.

Erosion failure of coated inserts was due to oxidation of the coating. In the case of a diffusion coating of silicon carbide, lack of continuous coating led to substrate oxidation, which hastened erosion failure. The combination gave less erosion protection than standard ablatives. The best pyrolytic graphite coating, which included boron codeposition, provided erosion protection for 140 seconds of continuous firing. In order to improve upon this coating, a more oxidation-resistant pyrolytic graphite must be developed. The other alternative is to use a thicker pyrolytic graphite-boron coating, if the structural problems of a thicker coating can be solved.

The preferentially oriented pyrolytic graphite insert gave erosion protection for 218 seconds of continuous firing. The best ablative nozzle of reference 1 gave no erosion for 118 seconds of continuous firing. The design goal of 300 seconds of erosion-

free operation is within reach if the structural problems can be solved without changing the erosion resistance significantly.

Silicon carbide can be used successfully in the test environment if run times are limited or wall temperatures are kept below the oxidation threshold. Insert 1 provided erosion protection for three 100-second firings in spite of structural failure. The heavy-wall heat-sink design and the short firing times were responsible. When a thin-wall silicon carbide insert was fired for 250 seconds continuously, its erosion rate due to oxidation matched the average erosion of ablative nozzles in reference 1. Tungsten infiltrated with copper gave the best erosion resistance for firing durations over 300 seconds. The throat area increase was 8 percent after a 340-second firing. This value compares with an 8 percent increase after 240 seconds for the best ablative nozzle of reference 1. Tungsten-silver provided the same erosion resistance, but structural failure cut short its test duration. Further improvements for the infiltrated tungsten might be made by varying the infiltrant composition and/or percentage. Of course, the high density of tungsten must be considered in any design.

Lewis Research Center,
National Aeronautics and Space Administration,
Cleveland, Ohio, August 15, 1967,
128-31-03-01-22.

APPENDIX - SYMBOLS

C_d	nozzle discharge coefficient (determined as in ref. 4), 0.994
D_e	rocket nozzle exit diameter, in.; cm
F	thrust, lb force; N
F_{vac}	vacuum thrust, $F + P_0 D_e^2 \pi/4$, lb force; N
I_{vac}	vacuum impulse, F_{vac}/w_p, sec
O/F	oxidant-fuel ratio, w_{ox}/w_f
P_c	chamber pressure measured at injector, psia; N/sq m
$P_{c, corr}$	corrected chamber pressure (total pressure at rocket throat) (determined as in ref. 4), φP_c, psia; N/sq m
P_0	altitude pressure surrounding engine, psia; N/sq m
ΔR_e	effective throat radius change, $R_t - R_i$, in.; cm
R_i	initial throat radius, in.; cm
R_t	throat radius, $\sqrt{\frac{\eta_{C^*} C^*_{theor} w_p}{\pi g P_{c, corr} C_d}}$, in.; cm
S.F.	safety factor, ratio of ultimate stress to maximum calculated stress
w_f	fuel weight flow; average, $(w_{f,1} + w_{f,2})/2$, lb/sec; kg/sec
w_{ox}	oxidant weight flow; average, $(w_{ox,1} + w_{ox,2})/2$, lb/sec; kg/sec
w_p	total propellant flow, $w_{ox} + w_f$, lb/sec; kg/sec
η_{C^*}	characteristic velocity efficiency, $\eta_{I_{sp}} / \eta_{C_F, vac}$
$\eta_{C_F, vac}$	vacuum thrust coefficient efficiency (determined as in ref. 4), 0.983
$\eta_{I_{sp}}$	impulse efficiency, $I_{vac}/I_{vac, theoretical\ equilibrium}$
φ	correction factor for measured pressure at injector to total pressure at throat (determined as in ref. 4), 0.946

Subscripts:

vac	vacuum
1	turbine meter 1
2	turbine meter 2

REFERENCES

1. Peterson, Donald A.: Experimental Evaluation of High-Purity-Silica Reinforced Ablative Composites as Nozzle Sections of 7.8-Inch- (19.8-cm) Diameter Throat Storable-Propellant Rocket Engine. NASA TM X-1391, 1967.

2. Winter, Jerry M.; Plews, Larry D.; and Johnston, James R.: Experimental Evaluation of Throat Inserts in a Storable-Propellant Rocket Engine. NASA TM X-1266, 1966.

3. Lynch, J. F.; Ungar, E. W.; Bowers, D. J.; and Duckworth, W. H.: Investigation of Nozzle-Failure Mechanisms and of Parameters Affecting Nozzle-Material Suitability in Solid-Propellant Rockets. (AFASD-TDR-63-738), Batelle Memorial Inst., Aug. 1963.

4. Shinn, Arthur M., Jr.: Experimental Evaluation of Six Ablative-Material Thrust Chambers as Components of Storable-Propellant Rocket Engines. NASA TN D-3945, June 1967.

5. Schultz, F. E.; and Cline, P. B.: Analytical Comparisons of Ablative Nozzle Materials. General Electric Co. (NASA CR-54257), July 1, 1965.

6. Au, Norman N.: Stresses and Strains in Multi-Layer Disks, Cylinders, and Spheres Under Pressure Loading and an Arbitrary Radial Temperature Gradient. Rep. No. TDR-269(4304)-2(SSD-TDR-63-227), Aerospace Corp., Oct. 1963.

7. Manson, S. S.: Thermal Stresses in Design. Part 5 - Interpretation of Fatigue Data for Ductile Materials. Machine Des., vol. 30, no. 18, Sept 4, 1958, pp. 126-133.

NASA-Langley, 1968 —— 28 E-4032

Motion-picture film supplement C-255 is available on loan. Requests will be filled in the order received. You will be notified of the approximate date scheduled.

The film (16 mm, 15 min, color, sound) shows three main failure mechanisms in the evaluation of throat inserts in a storable-propellant rocket engine: (1) oxidation, (2) thermal stress, and (3) delamination of layer planes.

Film supplement C-255 is available on request to:

Chief, Technical Information Division (5-5)
National Aeronautics and Space Administration
Lewis Research Center
21000 Brookpark Road
Cleveland, Ohio 44135

CUT

Date _____

Please send, on loan, copy of film supplement C-255 to
TM X-1463

_____

Name of Organization

_____

Street Number

_____

City and State Zip Code

Attention: Mr. _____

Title _____

Place
stamp
here

Chief, Technical Information Division (5-5)
National Aeronautics and Space Administration
Lewis Research Center
21000 Brookpark Road
Cleveland, Ohio 44135

"The aeronautical and space activities of the United States shall be conducted so as to contribute . . . to the expansion of human knowledge of phenomena in the atmosphere and space. The Administration shall provide for the widest practicable and appropriate dissemination of information concerning its activities and the results thereof."

—NATIONAL AERONAUTICS AND SPACE ACT OF 1958

NASA SCIENTIFIC AND TECHNICAL PUBLICATIONS

TECHNICAL REPORTS: Scientific and technical information considered important, complete, and a lasting contribution to existing knowledge.

TECHNICAL NOTES: Information less broad in scope but nevertheless of importance as a contribution to existing knowledge.

TECHNICAL MEMORANDUMS: Information receiving limited distribution because of preliminary data, security classification, or other reasons.

CONTRACTOR REPORTS: Scientific and technical information generated under a NASA contract or grant and considered an important contribution to existing knowledge.

TECHNICAL TRANSLATIONS: Information published in a foreign language considered to merit NASA distribution in English.

SPECIAL PUBLICATIONS: Information derived from or of value to NASA activities. Publications include conference proceedings, monographs, data compilations, handbooks, sourcebooks, and special bibliographies.

TECHNOLOGY UTILIZATION PUBLICATIONS: Information on technology used by NASA that may be of particular interest in commercial and other non-aerospace applications. Publications include Tech Briefs, Technology Utilization Reports and Notes, and Technology Surveys.

Details on the availability of these publications may be obtained from:

SCIENTIFIC AND TECHNICAL INFORMATION DIVISION

NATIONAL AERONAUTICS AND SPACE ADMINISTRATION

Washington, D.C. 20546